EFFECT OF HYDROLYSIS ON THE PROPERTIES OF A NEW VISCOELASTIC SURFACTANT-BASED ACID

A Thesis

by

ZHENHUA HE

Submitted to the Office of Graduate Studies of
Texas A&M University
in partial fulfillment of the requirements for the degree of

MASTER OF SCIENCE

Chair of Committee,	Hisham A. Nasr-El-Din
Committee Members,	Jerome J. Schubert
	Mahmoud El-Halwagi
Head of Department,	A. Daniel Hill

August 2013

Major Subject: Petroleum Engineering

ABSTRACT

Viscoelastic surfactants (VES) have been widely used in acidizing and acid fracturing. They are used as diversion agents during matrix acid treatments and leakoff control agents during acid fracturing. At high temperatures, viscoelastic surfactants hydrolyze, resulting in phase separation after a certain time. Their viscosities significantly decrease and it is much easier for them to flow back causing much less damage to the formation.

In this study, 4 to 8 wt% of a new VES-acid system was tested at temperatures of up to 250°F over hydrolysis times of 0 to 6 hours. Then, the solutions were neutralized by calcium carbonate until the pH reached 4.5. An HP/HT rheometer was used to measure the viscosity of the spent acids. Mass spectrometry (MS) was conducted to analyze the hydrolysis products of the VES. Coreflood tests were also conducted on Indiana limestone to determine the effects of the hydrolysis products on the permeability of these cores. The temperature was set at 250°F and the flow rate at 2.5 cm^3/s.

The viscosities of all VES-acid systems remained high at the beginning of hydrolysis, which was good for acid diversion. After that, the VES acid systems experienced a significant viscosity reduction due to phase separation; it became much easier for the spent acid to flow back. Coreflood experiments caused little damage to the Indiana limestone. MS results indicated hydrolysis of peptide bonds. Fatty acids formed the top oil layer, and amine-based molecules formed the aqueous phase.

This study will summarize and discuss the details of viscosity changes of the acid systems of this kind of viscoelastic surfactant, the damage caused by hydrolysis products, and how this kind of viscoelastic surfactant can be used to improve treatments.

DEDICATION

This thesis is dedicated to my grandparents, parents, and wife, who have supported and loved me all the time.

Also, this thesis is dedicated to my advisor, who has been a great source of motivation and inspiration.

Finally, this thesis is dedicated to all those who love life.

ACKNOWLEDGEMENTS

I would like to thank my committee chair, Professor Hisham A. Nasreldin, and my committee members, Dr. Shubert and Dr. El-Halwagi, for their instruction and support during this research.

I would also like to thank my colleagues, the department faculty and the staff for their help to make my study and research much easier and happier. My gratitude is also extended to all the Texas A&M teachers and students.

Finally, I would like to give thanks to my parents for their encouragement and to my wife for her patience and love.

NOMENCLATURE

C_A	Concentration of species A at the reactive surface
E_f	Reaction rate constant with units of moles
J	Undamaged formation productivity
Js	Productivity of the damaged well
k	Permeability of the undamaged zone
ks	Reduced permeability of the damaged zone
R_A	The rate of appearance of A, moles/sec
r_A	Surface area-specific reaction rate of A
re	Drainage radius
rs	Radius of the damaged zone
rw	Wellbore radius
s	Skin factor
S_B	Surface area of B
α	Order of the reaction
γ	Shear rate
ν	Apparent viscosity

TABLE OF CONTENTS

Page

ABSTRACT..……..ii

DEDICATION iv

ACKNOWLEDGEMENTS v

NOMENCLATURE....vi

TABLE OF CONTENTS vii

LIST OF FIGURES....ix

LIST OF TABLES xii

CHAPTER I INTRODUCTION AND RESEARCH OBJECTIVES 1

I.1 Carbonate Matrix Acidizing 1
I.1.1 Mineralogy of Carbonate Reservoirs 2
I.1.2 Acids Used in Carbonate Acidizing....3
I.1.3 Chemistry of Carbonate Matrix Acidizing....3
I.1.4 Reaction Kinetics 4
I.1.5 Productivity Enhancement 5
I.2 Applications of Viscoelastic Surfactant (VES) in the Oilfield 8
I.2.1 Introduction of VES 8
I.2.2 Applications in the Oilfield....12
I.3 VES Working Mechanism 17
1.4 Hydrolysis Research of VES....19
1.5 Research Objectives 20

CHAPTER II IMPACT OF HYDROLYSIS ON THE APPARENT VISCOSITY OF A NEW CLASS OF VISCOELASTIC SURFACTANT-BASED ACID 21

II.1 Hydrolysis Experiments of the New VES-Based Acid (no corrosion inhibitor) at 190°F 21
II.1.1 Materials 21
II.1.2 Experiment Procedures....21
II.1.3 Results and Discussion 26

Page

II.2 Comparison of the Properties Between New VES-Based Acid and Amido-Carboxybetaine Surfactant-Based Acid at 190°F....31
II.2.1 Amido-Carboxybetaine Surfactant....31
II.2.2 Results and Discussion....32
II.3 Hydrolysis Experiments of the New VES-Based Acid (with corrosion inhibitor) at 250°F....36
II.3.1 Materials....36
II.3.2 Experiment Procedures....37
II.3.3 Results and Discussion....39

CHAPTER III COREFLOOD EXPERIMENT ON FORMATION DAMAGE CAUSED BY HYDROLYSIS PRODUCTS....51

III.1 Materials....51
III.2 Experiment Procedures....51
III.3 Results and Discussion....53

CHAPTER IV CONCLUSIONS....60

REFERENCES....62

APPENDIX…....67

LIST OF FIGURES

Page

Fig. 1—Acid-carbonate minerals reaction kinetics. 5

Fig. 2—Sketch of a well with a near wellbore zone rs with altered permeability ks. 6

Fig. 3—Stimulation ratio changes with Xd (ratio of damaged permeability and undamaged permeability). 8

Fig. 4—Model of a surfactant molecule (Kefi et al. 2005). 9

Fig. 5—Four categories of surfactant based on hydrophilic heads. 10

Fig. 6—Chemical structure of amido-carboxybetaine surfactant. 11

Fig. 7—Schematic of a target zone with 2 subzones of different permeability. 13

Fig. 8—Schematic of a target zone being treated with acidizing method. 14

Fig. 9—Simplified sketch of ball sealer working mechanism. 15

Fig. 10—A schematic illustration of entangled wormlike micelles network (Yu et al. 2011). 18

Fig. 11—Water bath setup used for hydrolysis experiments of VES-Based acid at 190°F. 23

Fig. 12—Thermo scientific orion ross electrode. 24

Fig. 13—Centrifuge (Z206A from Labnet International). 25

Fig. 14—Grace instrument M5600 rheometer. 26

Fig. 15—Viscosity as a function of shear rates for 4 wt% VES-based acid (15 wt% HCl) at 190°F. 27

Fig. 16—Viscosity as a function of shear rates for 6 wt% VES-based acid (15 wt% HCl) at 190°F. 28

Fig. 17—Viscosity as a function of shear rates for 8 wt% VES-based acid (15 wt% HCl) at 190°F. 29

Fig. 18—Chemical structure of amido-carboxybetaine surfactant. 31

Page

Fig. 19—Comparison of viscosity change between 4 wt% new and old VES-based acid (15 wt% HCl) at 190°F. 33

Fig. 20—Comparison of viscosity change between 6 wt% new and old VES-based acid (15 wt% HCl) at 190°F. 34

Fig. 21—Comparison of viscosity change between 8 wt% new and old VES-based acid (15 wt% HCl) at 190°F. 35

Fig. 22—See-through cell used for hydrolysis experiments of VES-based acid at 250°F. 38

Fig. 23—Viscosity as a function of shear rates for 4 wt% VES-based acid (15 wt% HCl+ 1 vol% corrosion inhibitor) at 250°F, 300 psi. 39

Fig. 24—4 wt% VES-based acid sample after hydrolysis of 0, 0.25, 0.5, 1, 2, 3, 6 hours separately at 250°F. 40

Fig. 25—Viscosity as a function of shear rates for 6 wt% VES-based acid (15 wt% HCl+ 1 vol% corrosion inhibitor) at 250°F, 300 psi. 41

Fig. 26—6 wt% VES-based acid sample after hydrolysis of 0, 0.25, 0.5, 1, 2, 3, 6 hours separately at 250°F. 42

Fig. 27—Viscosity as a function of shear rates for 8 wt% VES-based acid (15 wt% HCl+ 1 vol% corrosion inhibitor) at 250°F, 300 psi. 43

Fig. 28—8 wt% VES-based acid sample after hydrolysis of 0, 0.25, 0.5, 1, 2, 3, 6 hours separately at 250°F. 44

Fig. 29—Viscosity as a function of different hydrolysis time for different concentration VES-based acid (15 wt% HCl+ 1 vol% corrosion inhibitor) at 100 s^{-1} at 250°F, 300 psi. 45

Fig. 30—Viscosity as a function of different hydrolysis time for different concentration VES-based acid (15 wt% HCl+ 1 vol% corrosion inhibitor) at 300 s^{-1} at 250°F, 300 psi. 46

Fig. 31—Hydrolysis reaction of (a) new VES into (b) fatty acid and (c) amine-based molecule. 47

Fig. 32—Diagram of MS spectrum of top layer substances after 6 hours hydrolysis at 250°F with the range of 10 to 500 m/z. 48

Page

Fig. 33—Diagram of MS spectrum of bottom layer substances after 6 hours hydrolysis at 250°F with the range of 10 to 500 m/z. 48

Fig. 34—The lower white part of the solution after 3 hours hydrolysis under the microscope, and it is highly conductive. 50

Fig. 35—Coreflood setup. 52

Fig. 36—Inlet and outlet face of the 6-inch Indiana limestone core before and after test with VES-based acid solution (heated 0 hour at 250°F). 54

Fig. 37—Pressure drop across the core during the coreflood test. 55

Fig. 38—Viscoelastic surfactant gel formed by 6 wt% VES-based acid after 0 hour hydrolysis and neutralization with calcium carbonate powder. 56

Fig. 39—Inlet and outlet face of the 6-inch Indiana limestone core before and after test with VES-based acid solution (heated 2 hour at 250°F). 58

Fig. 40—Pressure drop across the core during the coreflood test. 59

LIST OF TABLES

Page

Table 1—Composition of New VES-Based Acid Samples 22

Table 2—Composition of Old VES-Based Acid Samples 32

Table 3—Composition of New VES-Based Acid Samples 38

Table 4—Results of the Coreflood Expriments 56

Table 5—4 wt% VES-Based Acid Viscosity Changes with Different Hydrolysis Times at Different Shear Rates (190°F) 67

Table 6—6 wt% VES-Based Acid Viscosity Changes with Different Hydrolysis Times at Different Shear Rates (190°F) 68

Table 7—8 wt% VES-Based Acid Viscosity Changes with Different Hydrolysis Times at Different Shear Rates (190°F) 69

Table 8—4 wt% VES-Based Acid Viscosity Changes with Different Hydrolysis Times at Different Shear Rates (250°F, with Corrosion Inhibitor) 70

Table 9—6 wt% VES-Based Acid Viscosity Changes with Different Hydrolysis Times at Different Shear Rates (250°F, with Corrosion Inhibitor) 71

Table 10—8 wt% VES-Based Acid Viscosity Changes with Different Hydrolysis Times at Different Shear Rates (250°F, with Corrosion Inhibitor) 72

CHAPTER I

INTRODUCTION AND RESEARCH OBJECTIVES[*]

I.1 Carbonate Matrix Acidizing

Economides et al. (2000) indicated that matrix stimulation has been extensively used since the 1930s to improve the productivity of oil and gas wells and the injectivity of injection wells. Carbonate matrix acidizing is a technique in which acid systems are injected into formations at pressures below that which would cause fracturing, to create new, unimpaired flow channels between the wellbore and the carbonate formation. Its purpose is to increase the connectivity of a formation with the wellbore throughout the entire zone of interest.

The first attempt at using acids to stimulate oil wells of carbonate reservoirs was in 1895. At that time both hydrochloric and sulfuric acids were used for this purpose. Although several wells were treated, the process failed to arouse general interest due to severe corrosion of well casings and other metal equipment.

The next attempts to use acids occurred between 1925 and 1930. These were attempts of using hydrochloric acid (HCl) to dissolve scale in wells in the Glenpool field of Oklahoma and to increase production from the Jefferson Limestone (Devonian) in

---

[*] Parts of this chapter are reprinted with permission from "Hydrolysis Effect on the Properties of a New Class of Viscoelastic Surfactant-Based Acid and Damage Caused by the Hydrolysis Products" by Zhenhua He, Guanqun Wang, Hisham A. Nasr-El-Din, and Stuart Holt, 2013. Proceedings of SPE European Formation Damage Conference and Exhibition, Copyright [2013] by Society of Petroleum Engineers.

Kentucky. None of these efforts were successful, and acidizing was abandoned once again.

With the discovery of arsenic inhibitors in 1932, which allows hydrochloric acid to react with the carbonate formation without seriously damaging the well casing and other metal equipment, acidizing began to attract a lot of attention once more. In this period, the Pure Oil Company and the Dow Chemical Company successfully treated a limestone formation in Isabella County, MI with HCl and these inhibitors. Soon afterwards, similar treatments were done on the nearby wells, and the acidizing industry began to flourish.

Matrix acidizing operations are, now, a predominate treatment for carbonate wells around the world.

I.1.1 Mineralogy of Carbonate Reservoirs

Carbonate reservoirs hold more than 60% of oil and 40% of gas reserves worldwide. This is true especially in the Middle East, about 70% of oil and 90% of gas reserves are in carbonate formations. Carbonate fields play a dominant role in oil and gas reserves.

Carbonate reservoirs are primarily composed of calcite ($CaCO_3$), Dolomite ($CaMg(CO_3)_2$), Ankerite ($Ca(MgFeMn)(CO_3)_2$), and Chalk. Some natural fractures and vugs exist in them.

I.1.2 Acids Used in Carbonate Acidizing

I.1.2.1 Hydrochloric Acid

Hydrochloric acid is a commonly used acid in carbonate acidizing. Most of the minerals in carbonate reservoirs can be dissolved in hydrochloric acid, and the reaction products (calcium chloride, $CaCl_2$ and Magnesium chloride, $MgCl_2$ etc.) are soluble in water. Usually, 5 - 28 wt% HCl are employed in the field. However, HCl is highly corrosive to the tubular and the pump lines especially at high reservoir temperatures (above 250°F). Therefore corrosion inhibitors are needed when HCl is used.

I.1.2.2 Organic Acids

Yu et al. (2011) mentioned that organic acids such as formic acid and acetic acid are used in carbonate acidizing primarily because they are much less corrosive than HCl at high reservoir temperatures. 10 wt% acetic acid is often used. The reaction products of acetic acid and carbonate rocks (calcium acetates, $Ca(COOCH_2CH_3)_2$, and magnesium acetates, $Mg(COOCH_2CH_3)_2$) are soluble in water. However, acetic acid is much more expensive than HCl and formic acid. Formic acid is more corrosive than acetic acid, but effective inhibitors are available for formic acid at temperatures of up to 400°F.

I.1.3 Chemistry of Carbonate Matrix Acidizing

Carbonate reservoirs are mainly composed of calcite ($CaCO_3$), and dolomite ($CaMg(CO_3)_2$). The reactions of HCl, calcite, and dolomite are as follows,

$$2HCl + CaCO_3 \rightarrow CaCl_2 + H_2O + CO_2 \uparrow \quad (1.1)$$

$$4HCl + CaMg(CO_3)_2 \rightarrow CaCl_2 + MgCl_2 + 2H_2O + 2CO_2 \uparrow \quad (1.2)$$

HCl will completely dissociate to hydrogen ions, H^+, and chloride ions, Cl^- when it dissolves in water since it is a strong acid. The reaction between HCl and carbonate minerals is actually the reaction between the hydrogen ions and the carbonate minerals.

I.1.4 Reaction Kinetics

Economides et al. (2000) stated that acid-mineral reactions are heterogeneous reaction because the reactions occur at the interface of two or more different phases. The kinetics is the description of the reaction rate between an acid and the minerals. Once the acid molecules reach the surface of the minerals by diffusion or convection, the acid-mineral reaction begins. Therefore, acid-mineral reaction kinetics depends on two processes: (1) the rate of transport of acid molecules to the mineral surface by convection and diffusion; (2) the rate of acid reaction with the minerals (See **Fig. 1**). The overall reaction rate is controlled by the slower process. For example, the rate of acid reaction with the carbonates is much faster than the rate of transport of the acid molecules to the mineral surface, so the overall reaction rate is controlled by process (1).

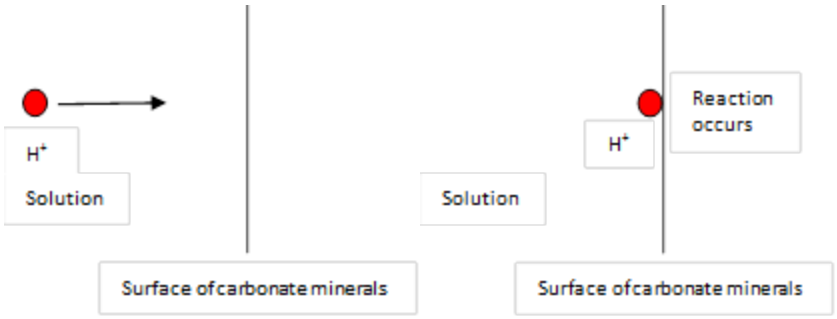

Fig. 1—Acid-carbonate minerals reaction kinetics.

$$R_A = r_A S_B \tag{1.3}$$

R_A— the rate of appearance of A, moles/sec;

r_A— surface area-specific reaction rate of A;

S_B— surface area of B.

$$-R_A = E_f C_A^{\alpha} S_B \tag{1.4}$$

E_f — reaction rate constant with units of moles A/[m^2 − sec− ($molesA/m^3$)$^{\alpha}$];

C_A— concentration of species A at the reactive surface;

α — order of the reaction.

I.1.5 Productivity Enhancement

Economides et al (1993) presented that carbonate matrix acidizing is a near wellbore treatment with all of the acid reacting within a few, to perhaps as much as ten feet of the wellbore in carbonates.

The productivity index of a well in an undersaturated reservoir is given as follows (The parameters are shown in **Fig. 2**):

$$J = \frac{q}{P_e - P_{wf}} = \frac{kh}{141.2\mu[\ln(r_e / r_w) + s]} \tag{1.5}$$

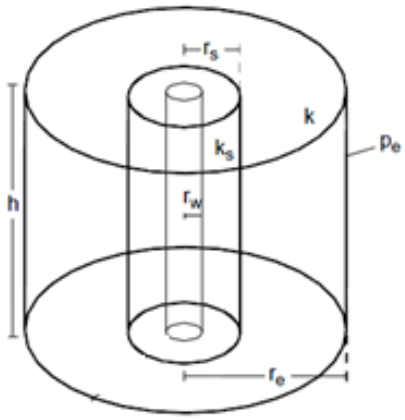

Fig. 2—Sketch of a well with a near wellbore zone rs with altered permeability ks.

So, the ratio of the stimulated productivity index to the damaged productivity index is as follows (Muskat 1949):

$$\frac{J_i}{J_d} = \frac{\ln(r_e / r_w) + s}{\ln(r_e / r_w)} \tag{1.6}$$

Note that when there is no damage near the wellbore, s is equal to 0.

Skin factor is related to the permeability and radius of the damaged region by Hawkins' formula mentioned in Petroleum Production Systems by Economides et al 1993.

$$s = (\frac{k}{k_s} - 1) \ln \frac{r_s}{r_w} \tag{1.7}$$

Substituting for s into the above equation gives the following:

$$\frac{J_i}{J_d} = 1 + (\frac{1}{X_d} - 1) \frac{\ln(r_s / r_w)}{\ln(r_e / r_w)} \tag{1.8}$$

Where X_d is the ratio of the damaged permeability to the undamaged permeability (k_s / k).

We assume that the well has a wellbore radius of r_w = 0.328 feet and a drainage radius of 745 feet; the stimulated damage radius r_s = 1 feet beyond the wellbore. X_d ranges from 0.05 to 1. Therefore, we can get the figure of stimulation ratio J_i / J_d change with the X_d.

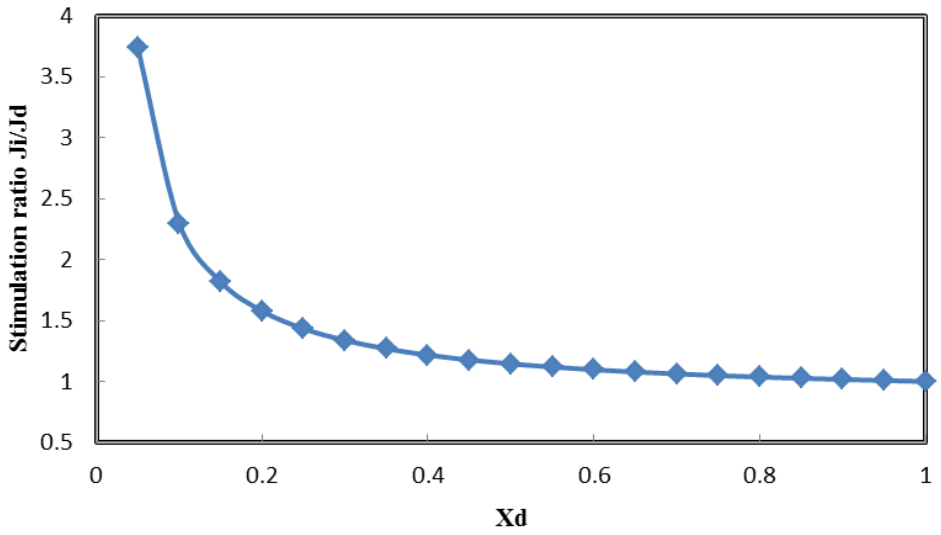

Fig. 3—Stimulation ratio changes with X_d (ratio of damaged permeability and undamaged permeability).

From **Fig. 3**, we can see that if the permeability of the damaged region is 5% of the original permeability, removal of the damage by the acidizing method can increase the productivity index by a factor of almost 4 times.

I.2 Applications of Viscoelastic Surfactant (VES) in the Oilfield

I.2.1 Introduction of VES

Surfactants are compounds that can lower the surface tension of a liquid, the interfacial tension between two liquids, or the interfacial tension between a solid and a liquid. Surfactants can work as detergents, foaming agents, emulsifiers, and dispersants. A surfactant usually has two components, one is a hydrophilic head group which is water soluble, the other one is a hydrophobic tail group which is water insoluble (oil soluble) (From Wikipedia). This is shown in **Fig. 4**.

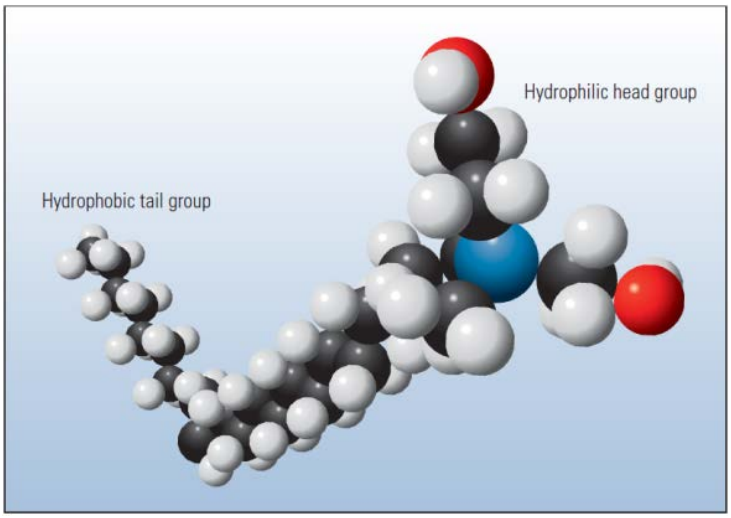

Fig. 4—Model of a surfactant molecule (Kefi et al. 2005).

Surfactants will diffuse in water. If water is in contact with air, the surfactant molecules will absorb at the interface between the water and air and the hydrophobic tails will extend into the air. If the water is in contact with oil, the surfactant molecules will absorb at the interface and the hydrophobic tails will extend into the oil.

In the aqueous phase, surfactants can form micelles when the concentration is above critical micelle concentration (CMC). The hydrophobic tails form the cores of the aggregates which are surrounded by the hydrophilic heads. The shape of the micelles can be spherical, wormlike, or bilayer, and it depends on the chemical structure of the surfactants and the balance between the sizes of the hydrophobic tails and hydrophilic heads.

Based on the hydrophilic head group of the different surfactants, they can be divided into four categories.

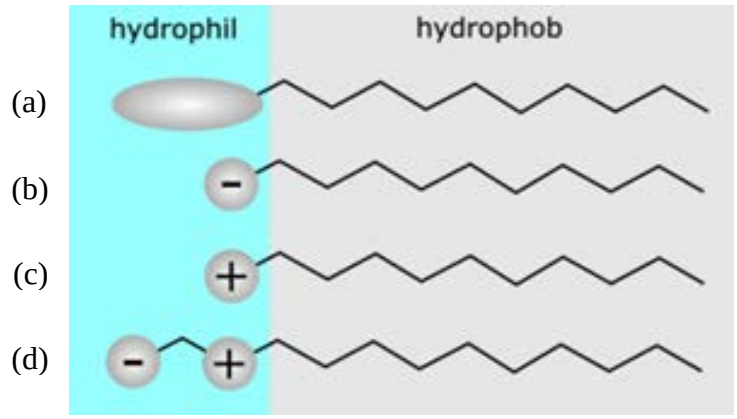

Fig. 5—Four categories of surfactant based on hydrophilic heads.

(1) Non-ionic: A non-ionic surfactant has no charged groups in its head. See **Fig. 5 (a)**. An example is cetyl alcohol. 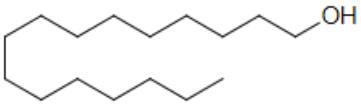

.

(2) Anionic: An anionic surfactant has negatively charged groups in its head. See **Fig. 5 (b)**. An example is sodium stearate.

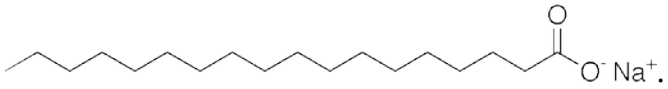

.

(3) Cationic: A cationic surfactant has positively charged groups in its head. See **Fig. 5 (c)**. An example is cetrimonium chloride.

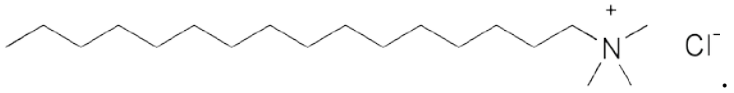

.

(4) Amphoteric: An amphoteric surfactant has both positively and negatively charged groups in its head. See **Fig. 5 (d)**. An example is cocamidopropyl betaine. 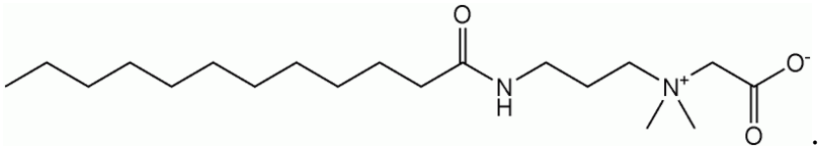

.

Viscoelasticity is the property of a material that can show viscous and elastic characteristics. Viscosity is the resistance to deformation by shear stress. For example, honey has a much higher viscosity than water. Elasticity is the property of a substance that causes the substance to return to its original state after stress on it has been removed (From Wikipedia).

VES molecules usually have long carbon chains (typically, 18-22 carbon atoms) as hydrophobic tails. For example, amido-carboxybetaine surfactant is commonly used in the oilfield. Its chemical structure is shown in **Fig. 6**.

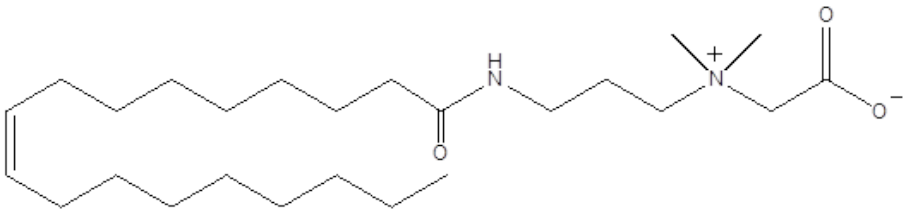

Fig. 6—Chemical structure of amido-carboxybetaine surfactant.

I.2.2 Applications in the Oilfield

In the petroleum industry, from 1977 viscoelastic surfactants started to be applied in matrix acidizing and fracturing treatments (Jahnke 1977; Syrinek et al. 1991). In the recent decade, viscoelastic surfactants have been widely and successfully used in acidizing (Nasr-El-Din et al. 2003; Zeiler et al. 2004), acid fracturing (Nasr-El-Din et al. 2003; Al-Muhareb et al. 2003; Artola et al. 2004; Bustos et al. 2007; Fontana et al. 2007; Bulat et al. 2008), and hydraulic fracturing jobs (Samuel et al. 1997). Usually, polymer-based acid systems will cause high friction pressures and formation damage because of residue precipitation, breakers are needed to enhance polymer degradation and make the flow back easier, and the cleanup time is lengthy. Viscoelastic surfactants were introduced to overcome these shortcomings.

The reaction between HCl and carbonate minerals is actually the reaction between the hydrogen ions and the carbonate minerals. Results of the reaction are mainly increase of pH and concentrations of the divalent cations (e.g. Ca^{2+}, Mg^{2+} etc.). When the pH and the divalent cations' concentrations reach the critical values, viscoelastic surfactant forms worm-shaped micelles and these micelles entangle with each other that lead the fluid to exhibit viscoelastic behavior (Samuel et al. 1997). This kind of micelle can be formed by individual surfactants with certain molecular structures which greatly increase their viscosity (Yang 2002). Therefore, it is very helpful for acid diversion or proppant suspension and placement. For matrix acid treatment, the acid will also be diverted to the low-perm zone and much more even distribution of acid in the

reservoir could be achieved. Much deeper penetration in the low-perm zone could significantly increase the permeabilities.

As mentioned above, VES has many applications in the oilfield. However, the following are its three most important applications.

I.2.2.1 Acid Diversion Agents

The success of a matrix acidizing job, to a large extent, depends on whether acid systems are distributed uniformly in the target interval. Many field experiences have shown that if there is no proper diversion method, satisfactory acid coverage cannot be assured. In **Fig. 7**, the permeability of subzone 1 is much greater than that of subzone 2. When acid system is injected, it is much easier for it to go through the subzone 1, leaving most of subzone 2 untreated as shown in **Fig. 8**.

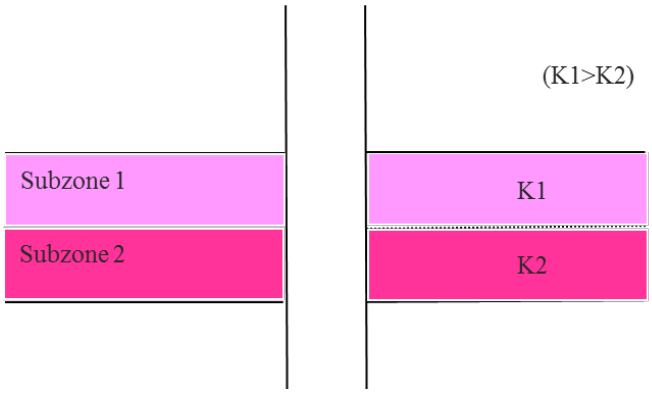

Fig. 7—Schematic of a target zone with 2 subzones of differing permeability.

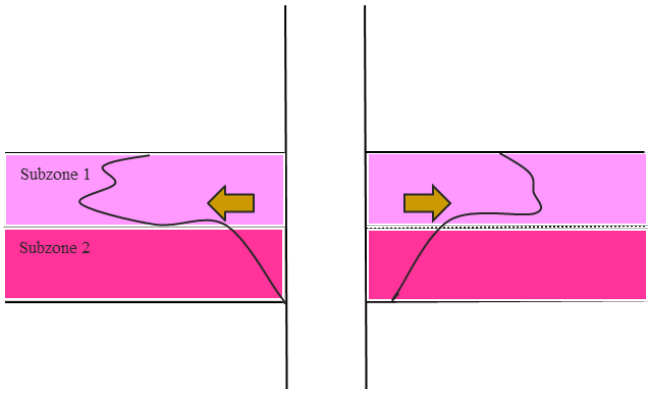

Fig. 8—Schematic of a target zone being treated with the acidizing method.

In general, diversion methods can be divided into either mechanical or chemical means. Mechanical control of treating fluid placement can be accomplished by coiled tubing with an inflatable packer, with conventional straddle packers, or with ball sealers (see **Fig. 9**). They have some obvious disadvantages: (1) They are expensive, (2) They are time consuming, (3) They are, often, not applicable or effective in wells with open-hole completions, (4) They only divert acids from the wellbore. However, when acids enter the formation, there is no control on their flow inside the formation.

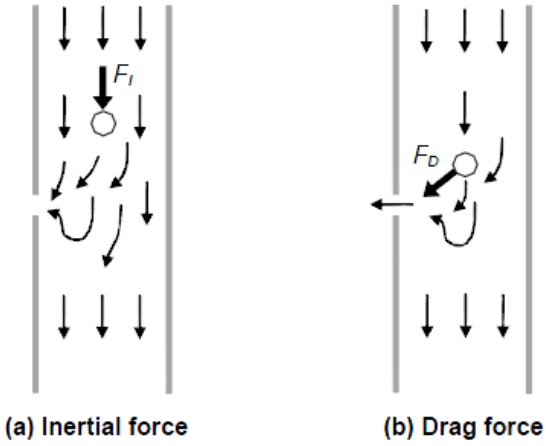

Fig. 9— Simplified sketch of a ball sealer working mechanism.

Chemical diversion can be achieved by using a viscous fluid, foam, or gel to lower the penetration of treatment fluid in the created wormholes and their surrounding matrix, or a particulate carrying fluid, which creates a filter cake on the surface of the wormholes. This filter cake results in the creation of a temporary skin which alters the injection profile. Gelled and foamed acids are also being used as a means of improving acid placement by combining stimulation and diversion in one step. High viscous, VES-based fluids can help divert and distribute the acid in the formation much more evenly so that the sweep efficiency and the acidizing effects are greatly enhanced.

I.2.2.2 Leakoff Control Agents

In acid fracturing jobs, the acid fluid is injected into the formation at pressures above the fracturing pressure, and many fractures are created. Low viscosity acid fluids will easily leakoff into the formation through the fractures. Highly viscous fluid can

prevent the acid leakoff into the formation. More acid will contribute to the penetration of fractures into the formation. The penetration distance will be much longer.

I.2.2.3 Proppant Suspension Agents

In hydraulic fracturing jobs, after the fractures are created, proppants will be injected into the formation to prop the fractures open so that the fractures will not close under the overburden pressure after the treatment. However, if the fluid used to transport the proppants has low viscosity, the proppants may precipitate at the bottom of the wellbore or at the entrance to the fractures. Highly viscous VES fluid would help to distribute the proppants much more uniformly in the fractures, and this would greatly enhance the conductivity of the fractures.

Many factors can affect the apparent viscosity of viscoelastic surfactants. Li et al. (2010, 2011) have investigated the impact of acid additives, Fe (III), organic acid and chelating agent on the apparent viscosity of amidoamine-oxide surfactant. At reservoir conditions, VES molecules tend to hydrolyze because of high temperatures and the fluid viscosity will be affected. In aqueous solutions, peptide bonds (-CO-NH-) in the surfactants can be easily broken in acidic environments at high temperatures, which is referred as acidic hydrolysis reaction (Long and Truscott 1968; Qian et al. 1993). Yu et al. (2012) used both experimental methods and molecular dynamics simulation studies to investigate the impact of hydrolysis on the apparent viscosity of carboxy-betaine viscoelastic surfactant. Peptide bonds within the viscoelastic surfactant molecules were cleaved and smaller molecules were generated, which led to viscosity being changed.

In this research, another VES-based acid system was hydrolyzed at 190 and 250°F, respectively. The partially spent acids (pH 4.5) (Fu and Chang 2005, 2006) kept high and stable viscosities for a certain time, and a significant viscosity reduction occurred later. This indicated that we may not need to add breakers.

I.3 VES Working Mechanism

If the concentration of the surfactant is above the critical micelle concentration (CMC), the hydrophobic tails of the surfactants will aggregate inside, leaving the hydrophilic heads outside to form a spherical micelle. When the acid in the solutions reacts with carbonate rock, the pH and the concentrations of the divalent cations, such as the Ca^{2+} and Mg^{2+}, increase. The spherical micelles will further develop into worm-like micelles, and they entangle with each other to form 3D network structures. This will greatly increase the viscosity of the fluid. A schematic illustration is shown in **Fig. 10.**

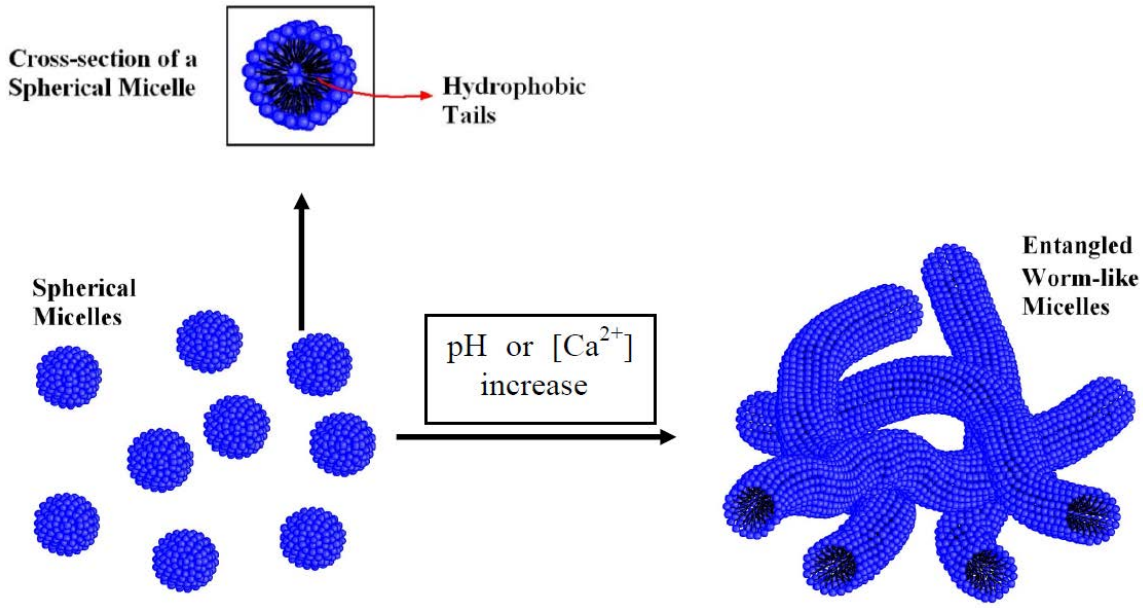

Fig. 10—A schematic illustration of an entangled wormlike micelles network (Yu et al. 2011).

Actually various chemicals have been developed to increase the viscosity of the injected fluids. Depending on the viscosifying agents, the fluids primarily can be divided into two categories: polymer-based fluids and surfactant-based fluids.

However, from research in recent decades, some obvious disadvantages have been found for the polymer-based fluids.

In-situ gelled acids which are composed of an acid, a polymer, a buffer, a breaker, and other additives are able to form a viscous gel in a narrow pH range (Yeager and Shuchart 1997; Taylor and Nasr-El-Din 2003), therefore, acid diversion can be achieved. But there are some drawbacks.

(1) Polymer retention and loss of permeability in tight carbonate cores (Taylor and Nasr-El-Din 2002; 2003);

(2) Precipitation of the crosslinker (Fe(III)) in tight carbonate cores at high temperatures (Lynn and Nasr-El-Din, 2001);

(3) Precipitation of the crosslinker (Fe(III)) in sour environments (Nasr-El-Din et al. 2002);

(4) Consumption of hydrogen sulfide (H_2S) scavengers by reacting with the polymer (Nasr-El-Din and Al-Humaidan, 2001).

VES-based acids were introduced to mitigate these problems caused by polymer-based fluids.

1.4 Hydrolysis Research of VES

In 2005, Fu and Chang observed that a type of amido-carboxybetaine surfactant-based acid fluid experienced a viscosity reduction when the samples were heated to 88°C. As an example, the sample with 4% HCl and 7.5 vol% surfactant was viscous in the first hour, became less viscous after 90 minutes of hydrolysis, and phase separation occurred at 180 minutes of hydrolysis.

In 2011, Yu et al. did a systemic study on the impact of hydrolysis at 190°F on the apparent viscosity of amido-carboxybetaine surfactant with both experimental and molecular dynamics (MD) simulation methods. She found that for all the samples with 15 wt% HCl and 4, 6, and 8 wt% surfactant that were partially spent (pH 4.5), maximum viscosity was obtained after 1 hour of hydrolysis. A significant viscosity reduction occurred after 3 hours of hydrolysis, and phase separation occurred. MD simulation showed that the optimum surfactant molar ratio was nearly 3:1 at which the worm like micelle structure was formed.

In our study, the impact of hydrolysis, at 190°F and 250°F, on the apparent viscosity of a new viscoelastic surfactant-based acid was studied and the potential formation damage caused by the hydrolysis products was measured.

1.5 Research Objectives

- The first objective of this research is to study the impact of hydrolysis on the apparent viscosity of this new VES-based acid (VES concentration from 4 wt% to 8 wt%) at 190°F and varying hydrolysis times (0-6 hours) and compare the viscosity change with hydrolysis time between this new VES-based acid and amido-carboxybetaine surfactant-based acid at 190°F.
- The second objective is to study the impact of hydrolysis on the apparent viscosity of this new VES-based acid (VES concentration from 4 wt% to 8 wt%) at 250°F and different hydrolysis times (0-6 hours).
- The last objective is to evaluate the potential formation damage caused by the hydrolysis on the permeability change of carbonate cores at 250°F.

CHAPTER II

IMPACT OF HYDROLYSIS ON THE APPARENT VISCOSITY OF A NEW CLASS OF VISCOELASTIC SURFACTANT-BASED ACID[*]

II.1 Hydrolysis Experiments of the New VES-Based Acid (no corrosion inhibitor) at 190°F

II.1.1 Materials

The materials used in this study are the VES sample (used as received), hydrochloric acid (ACS reagent grade, 36.66%), and calcium carbonate powder (ACS reagent grade, 99.95 wt%). All of the samples were prepared with de-ionized water (resistivity = 18.2 MΩ·cm at 25°C).

II.1.2 Experiment Procedures

1. VES-based acid solutions were prepared such that the HCl concentration was 15 wt% and the VES concentrations were 4, 6, and 8 wt%, respectively (**Table 1**).

[*] Parts of this chapter are reprinted with permission from "Hydrolysis Effect on the Properties of a New Class of Viscoelastic Surfactant-Based Acid and Damage Caused by the Hydrolysis Products" by Zhenhua He, Guanqun Wang, Hisham A. Nasr-El-Din, and Stuart Holt, 2013. Proceedings of SPE European Formation Damage Conference and Exhibition, Copyright [2013] by Society of Petroleum Engineers.

Table 1—COMPOSITION OF NEW VES-BASED ACID SAMPLES

Composition	Concentration of new VES		
	4 wt%	6 wt%	8 wt%
New VES	10 wt%	15 wt%	20 wt%
36.7 wt% HCl	41 wt%	41 wt%	41 wt%
DI water	49 wt%	44 wt%	39 wt%

2. Immediately after the solutions were prepared, they were put in the water bath setup (see **Fig. 11**) at 190°F. The hydrolysis times were set at 0.25, 0.50, 0.75, 1, 2, 3 and 6 hours. In the water bath setup, a return pipe was used. A thermometer was inserted into the water to monitor the temperature change of the water bath, and the heater was adjusted to make sure that the temperature remained stable at 190°F.

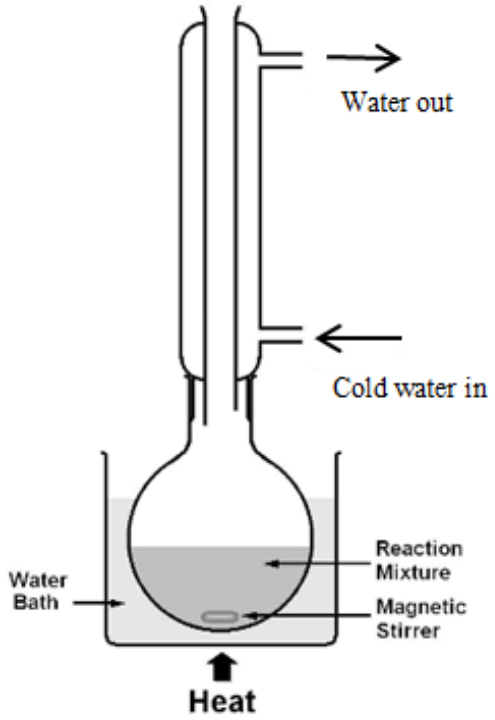

Fig. 11—Water bath setup used for hydrolysis experiments of VES-based acid at 190°F.

3. The samples were cooled down to room temperature and partially spent using calcium carbonate powder until their pH reached 4.5. A Thermo Scientific Orion Ross electrode (**Fig. 12**) was used to measure the pH of the spent acids. Before being used, this equipment needed to be calibrated with two calibration fluids.

Fig. 12—Thermo scientific orion ross electrode.

4. They were centrifuged for 40 minutes at 3,000 rpm (Z206A from Labnet International (**Fig. 13**)) to remove all of the bubbles and extra calcium carbonate powder. The difference in the weights of the two corresponding tubes in the rotating disk did not exceed 0.5 grams.

Fig. 13—Centrifuge (Z206A from Labnet International).

5. The spent acids were placed in the Grace Instrument M5600 HPHT Rheometer (**Fig. 14**) to measure their viscosity at various shear rates from 0.1 to 935.33 s^{-1}.

Fig. 14—Grace instrument M5600 rheometer.

Also, control experiments were conducted on the solutions with the same compositions and procedures, but they did not experience hydrolysis at 190°F.

II.1.3 Results and Discussion

II.1.3.1 Impact of Hydrolysis at 190°F on the Apparent Viscosity of the New VES-Based Acid

Fig. 15 shows the trend of the 4 wt% VES-based acid viscosity changes with the shear rates under hydrolysis of 0, 1, 2, and 3 hours at 190°F. (See more data for 4 wt% VES-based acid in **Table 5** in Appendix).

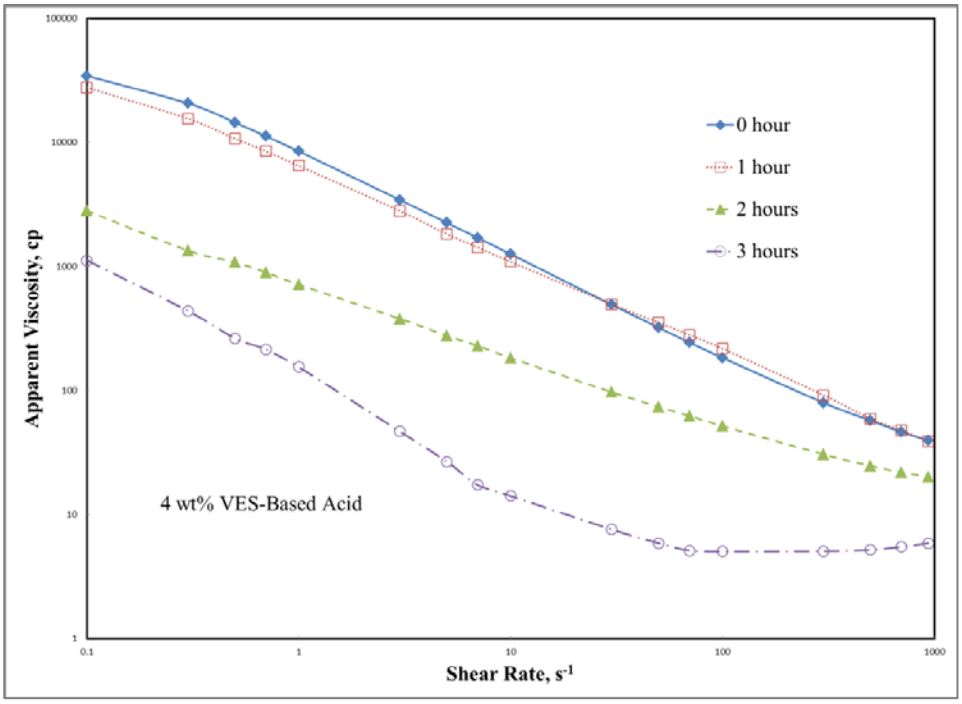

Fig. 15—Viscosity as a function of the shear rates for 4 wt% VES-based acid (15 wt% HCl) at 190°F.

In a Log-log scale coordinate, viscosities change linearly with the shear rate for the fluids, because they are power-law fluids. The equation of power-law fluids is as follows:

$$\nu = k\gamma^{n-1} \tag{2.1}$$

The values of Log(ν) and Log(γ) have a linear relationship. As shown in Fig. 15, during the first hour of hydrolysis, the viscosities of the 4 wt% VES-based acids did not change much. They remained relatively stable and high at about 1220, 330, 200, and 85 cp for 10, 50, 100, and 300 s^{-1}, respectively. When the viscosities are stable and high, acid diversion is helpful to make the acid distribute throughout the reservoir more evenly. After 2 hours of hydrolysis, the viscosities decreased suddenly. However, still

they were a little bit too high to be easy to flow back. These viscosities were 183, 74, 52, and 31 cp at 10, 50, 100, and 300 s^{-1}, respectively. At 3 hours of hydrolysis, all of the viscosities reduced to below 10 cp. It was easier for the fluid to flow back at such low viscosities.

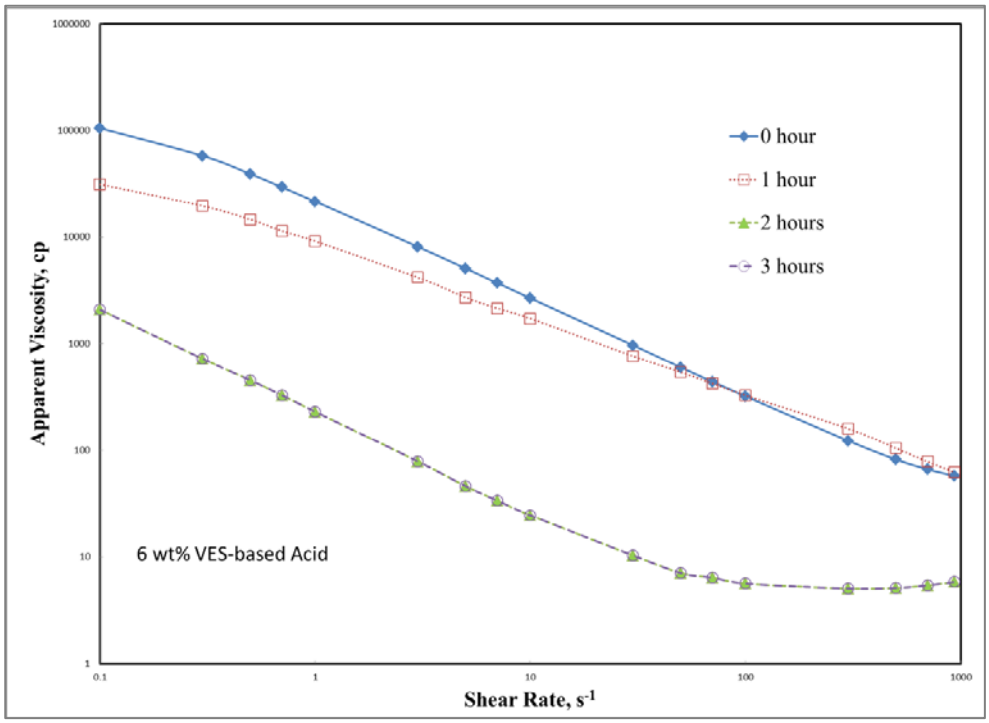

Fig. 16—Viscosity as a function of the shear rates for 6 wt% VES-based acid (15 wt% HCl) at 190°F.

Fig. 16 shows the trend of 6 wt% VES-based acid viscosity changes with shear rates under hydrolysis of 0, 1, 2, and 3 hours at 190°F. (See more data for 6 wt% VES acid system in **Table 6** in Appendix.) During the first hour of hydrolysis, compared with 4 wt% VES-based acid, the viscosities changed slightly more, but remained

relatively stable and high. They are about 2200, 550, 300, and 130 cp at 10, 50, 100, and 300 s^{-1}, respectively. Unlike 4 wt% VES-based acid, the viscosities suddenly decreased significantly to around 10 cp at 2 hours of hydrolysis, which was one hour earlier. It is easy to flow back after this.

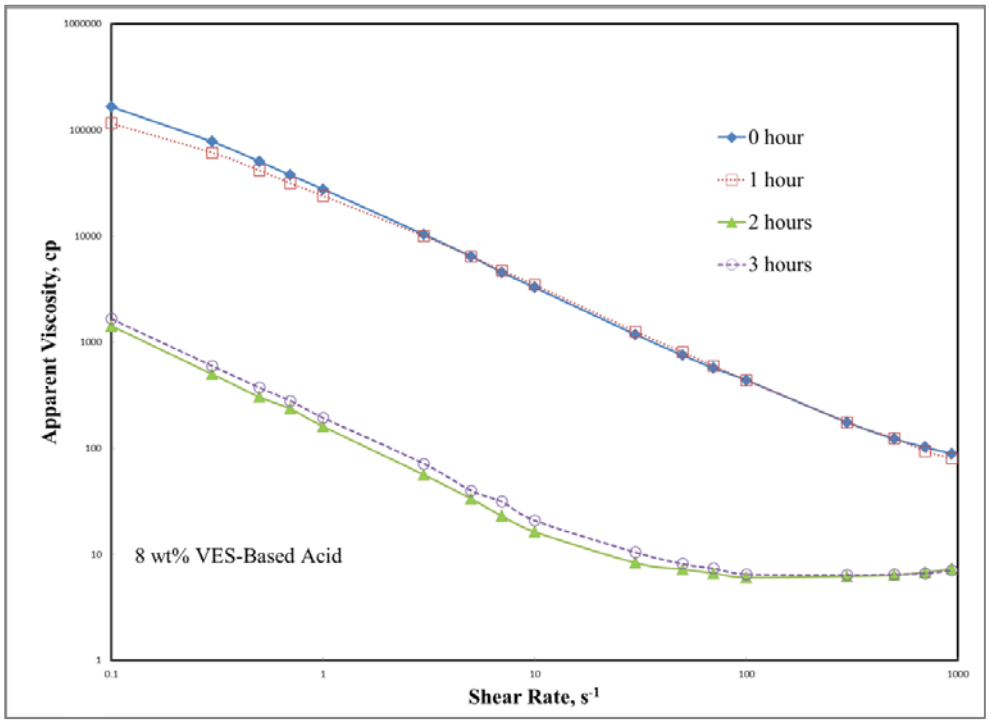

Fig. 17—Viscosity as a function of the shear rates for 8 wt% VES-based acid (15 wt% HCl) at 190°F.

Fig. 17 shows the trend of 8 wt% VES-based acid viscosity change with shear rates under hydrolysis of 0, 1, 2, and 3 hours at 190°F. (See more data for 8 wt% VES acid system in **Table 7** in Appendix.) From Fig. 17, similarly as 4 wt% and 6 wt% VES-based acids, the viscosities didn't change a lot between 0-hour and 1- hour

hydrolysis, and it changed even less for 8 wt% VES-based acid. The viscosities during the first hour hydrolysis remained relatively high. They are 3500, 800, 300, and 130 cp at 10, 50, 100, and 300 s^{-1}, respectively. This was beneficial for the acid diversion. Significant viscosity reduction occurred after 2 hours of hydrolysis and the viscosities fell below 10 cp.

From Figs. 15-17, generally, the viscosity of the new VES-based acid remained high and stable during the first hour of hydrolysis. There are two possible reasons this phenomena happened. The first is that the concentration of the viscoelastic surfactant is above the critical micelle concentration (CMC), above which long wormlike micelles are formed and they entangle with each other to construct a 3D network structure. The other reason is that, the fatty acids, produced from the hydrolysis reaction, co-assemble with the viscoelastic surfactant molecules to form worm like micelles under the influence of some metal ions. Also, these wormlike micelles will further develop into 3D network structures. This structure makes the solution much more viscous. This is very beneficial to divert and distribute the acids more evenly in the target formation and greatly enhances the sweep efficiency and acidizing effects.

After 2-3 hours of hydrolysis, the viscosity of the new VES-based acid significantly declined. As hydrolysis went on, the concentration of the viscoelastic surfactant became progressively smaller and at some point it was below the threshold concentration and was not concentrated enough to form wormlike micelles and later, the 3D network structure. The structure that made the solution viscous did not exist any longer so the viscosity significantly decreased. This is beneficial for flow back of the

treatment fluid after acidizing jobs. If the viscosity is small, it is easier for the fluid to flow back, and it causes much less friction.

II.2 Comparison of the Properties Between New VES-Based Acid and Amido-Carboxybetaine Surfactant-Based Acid at 190°F

II.2.1 Amido-Carboxybetaine Surfactant

Amido-carboxybetaine surfactant (also referred to as old VES in the following content) is one kind of amphoteric surfactant that has been used in carbonate matrix acidizing for a long time. Its chemical structure is shown in **Fig. 18**. Next we will do a comparison of viscosity change with hydrolysis times between amido-carboxybetaine surfactant-based acid and the new VES-based acid.

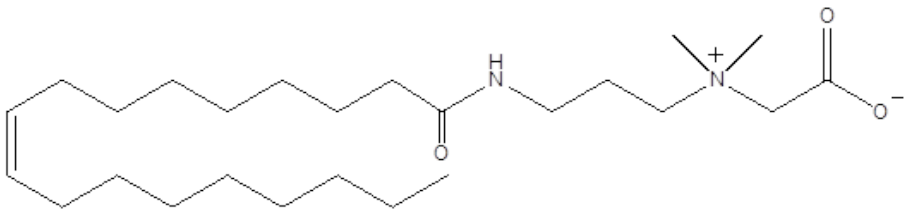

Fig. 18—Chemical structure of amido-carboxybetaine surfactant.

In 2011, Yu et al. researched the impact of hydrolysis at 190°F on the apparent viscosity of amido-carboxybetaine surfactant-based acid with both experimental and MD simulation methods. One of her conclusions about the properties of this kind of viscoelastic surfactant was that for all samples with 15 wt% HCl and 4, 6, and 8 wt%

amido-carboxybetaine surfactant that were hydrolyzed at 190°F and partially spent (pH 4.5), the maximum apparent viscosity was obtained after 1 hour of hydrolysis. A significant viscosity reduction occurred after 3 hours of hydrolysis.

II.2.2 Results and Discussion

Table 2—COMPOSITION OF OLD VES-BASED ACID SAMPLES

Composition	Concentration of old VES		
	4 wt%	6 wt%	8 wt%
Old VES	13 wt%	20 wt%	27 wt%
36.7 wt% HCl	41 wt%	41 wt%	41 wt%
DI water	46 wt%	39 wt%	32 wt%

Table 2 shows the composition of the old VES-based acid solutions. New VES-based acid composition is shown in Table 1.

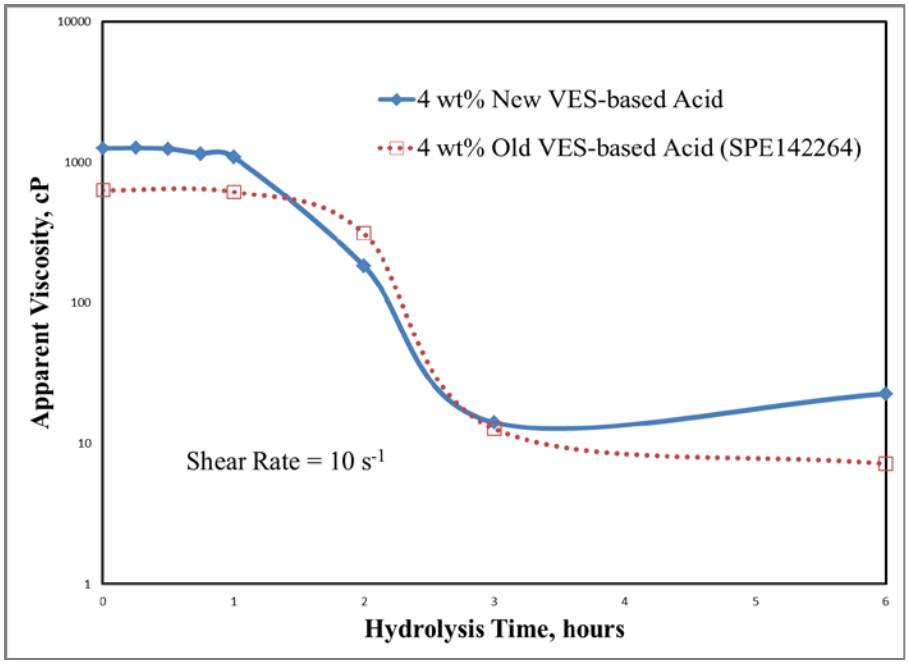

Fig. 19—Comparison of viscosity change between 4 wt% new and old VES-based acid (15 wt% HCl) at 190°F.

Fig. 19 shows the comparison of viscosity change between 4 wt% new and old VES-based acids (15 wt% HCl) at 190°F and shear rate of 10 s^{-1}. We can see from the figure that the viscosity of the old VES-based acid was fairly constant at about 800 cp in the first hour hydrolysis. For the new VES-based acid, the viscosity at the time points of 0.25, 0.50, and 0.75 hour were also measured. The viscosity of the new VES-based acids remained around 1200 cp during the first hour hydrolysis. It was higher than the old VES-based acid in this time period. Significant viscosity reduction occurred at 3 hours hydrolysis for both the old and new VES-based acids.

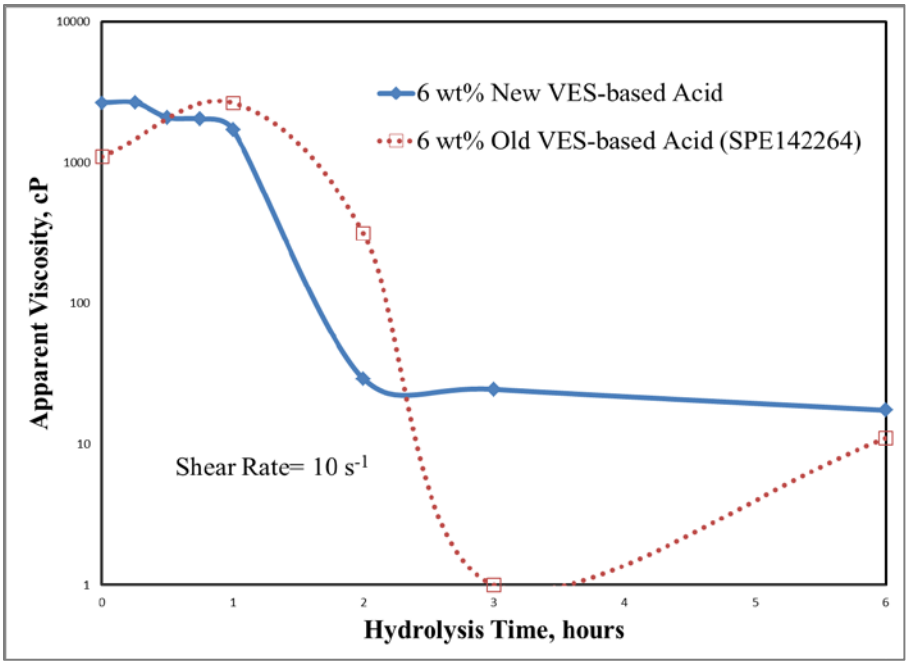

Fig. 20—Comparison of viscosity change between 6 wt% new and old VES-based acid (15 wt% HCl) at 190°F.

Fig. 20 shows the comparison of viscosity change between 6 wt% new and old VES-based acids (15 wt% HCl) at 190°F and shear rate of 10 s^{-1}. For the old VES-based acid, the viscosity gradually increased to its maximum value of around 2200 cp in the first hour and then decreased. Significant viscosity reduction occurred at 3 hour hydrolysis. For the new VES-based acid, the viscosity slightly decreased but was fairly constant at around 1500 cp during the first hour hydrolysis. Significant viscosity reduction occurred when it hydrolyzed for 2 hours.

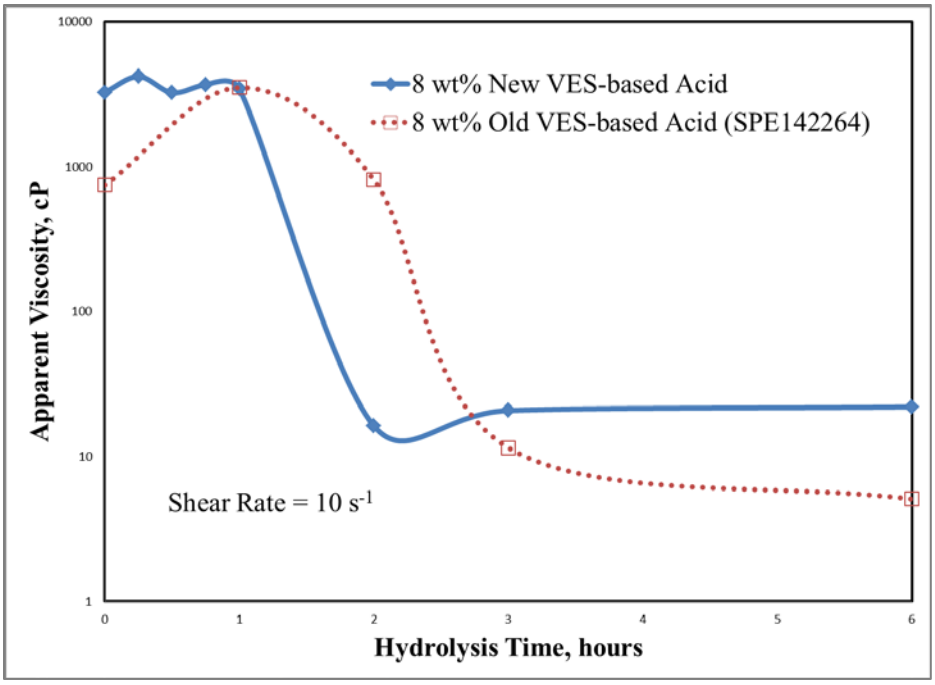

Fig. 21—Comparison of viscosity change between 8 wt% new and old VES-based acid (15 wt% HCl) at 190°F.

Fig. 21 shows the comparison of viscosity change between 8 wt% new and old VES-based acids (15 wt% HCl) at 190°F and shear rate of 10 s^{-1}. Similarly, 6 wt% old VES-based acid in the first hour of hydrolysis, the viscosity gradually increased to a maximum of around 3200 cp and then declined. It significantly decreased at 3 hours hydrolysis. For the new VES-based acid in the first hour hydrolysis, the viscosity fluctuated slightly around 3200 cp, which is the maximum viscosity of the 6 wt% old VES-based acid, and then fell down. It significantly declined at about 2 hours of hydrolysis.

Based on above, we can summarize that, for all samples with 15 wt% HCl and 4, 6, and 8 wt% viscoelastic surfactant that were hydrolyzed at 190°F and partially spent

(pH 4.5), the viscosity gradually built up to the maximum value during the first hour of hydrolysis for the old VES-based acid, while the viscosity remained high and fairly stable during the first hour of hydrolysis for the new VES-based acid. Significant viscosity reduction occurred at 3 hours hydrolysis for the old VES-based acid and this occurred in 2-3 hours hydrolysis for the new VES-based acid.

The reasons for the stable and high viscosity for the new VES-based acid is as mentioned above in the previous discussion section. Significant viscosity reduction occurred a little earlier for the new VES-based acid than the old VES-based acid. The first step for peptide bond hydrolysis is that hydrated hydrogen ions go to the peptide bonds. The hydrophilic head of the old VES molecule has one positive charge while the hydrophilic head of the new VES molecule has 0 charges. Therefore, it is much easier for the hydrated hydrogen ions to migrate to the peptide bonds of the new VES molecules than the old ones and it is a little faster for the new VES to hydrolyze.

II.3 Hydrolysis Experiments of the New VES-Based Acid (with corrosion inhibitor) at 250°F

II.3.1 Materials

The materials used in this study were the VES sample (used as received), hydrochloric acid (ACS reagent grade, 36.7%), a corrosion inhibitor, and calcium carbonate powder (ACS reagent grade, 99.95 wt%). All samples were prepared with de-ionized water (resistivity=18.2 MΩ·cm at 25°C).

II.3.2 Experiment Procedures

1. VES-based acid solutions were prepared such that the HCl concentration was 15 wt%, the corrosion inhibitor was 1 vol% and the VES concentrations were 4, 6, and 8 wt%, respectively (**Table 3**).
2. Immediately after the solutions were prepared, they were put in the see-through cell (**Fig. 22**) at 250°F. The hydrolysis times were set at 0.25, 0.50, 1, 2, 3, and 6 hours. The temperature of the see-through cell can be controlled by a temperature control device. The small window in the see-through cell wall is helpful to observe the samples inside.
3. The samples were cooled down to room temperature and partially spent by calcium carbonate powder until their pH reached 4.5.
4. They were centrifuged for 40 minutes at 3,000 rpm to remove all the bubbles and extra calcium carbonate powder.
5. The spent acids were placed in the Grace 5600 rheometer to measure their viscosity at various shear rates from 0.1 to 935.33 s^{-1}.

Also control experiments were conducted on the solutions with the same compositions and procedures, but they did not experience hydrolysis at 250°F.

Table 3—COMPOSITION OF NEW VES-BASED ACID SAMPLES

Composition	VES-Based Acid, g		
	4 wt%	6 wt%	8 wt%
VES	10	15	20
36.7 wt% HCl	41	41	41
DI water	49	44	39
Corrosion Inhibitor	1 vol%	1 vol%	1 vol%

Fig. 22—See-through cell used for hydrolysis experiments of VES-based acid at 250°F.

II.3.3 Results and Discussion

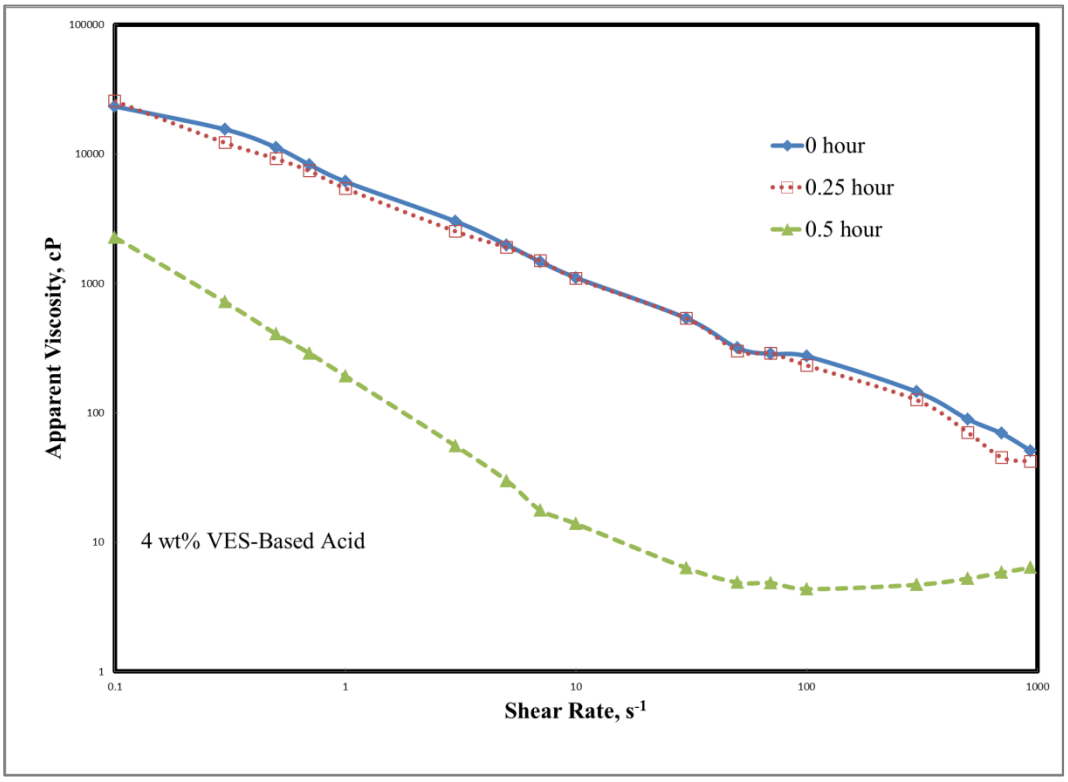

Fig. 23—Viscosity as a function of shear rates for 4 wt% VES-based acid (15 wt% HCl+ 1 vol% corrosion inhibitor) at 250°F, 300 psi.

Fig. 23 shows the trend of the 4 wt% new VES-based acid viscosity change with shear rates under hydrolysis of 0, 0.25, and 0.5 hour at 250°F. (See more data for 4 wt% VES-based acid in **Table 8** in Appendix). From Fig. 23, the viscosities remain stable and high during the 0.25 hour. For shear rates of 10, 50, 100, and 300 s^{-1}, their viscosities remained at about 1100 cp, 310 cp, 250 cp and 140 cp, respectively. Relatively high viscosity is helpful for acid diversion. After that, the viscosities decreased significantly. After 0.5 hour, their viscosities declined to below 5 cp. It was

easy for the fluid to flow back at low viscosities after the treatment.

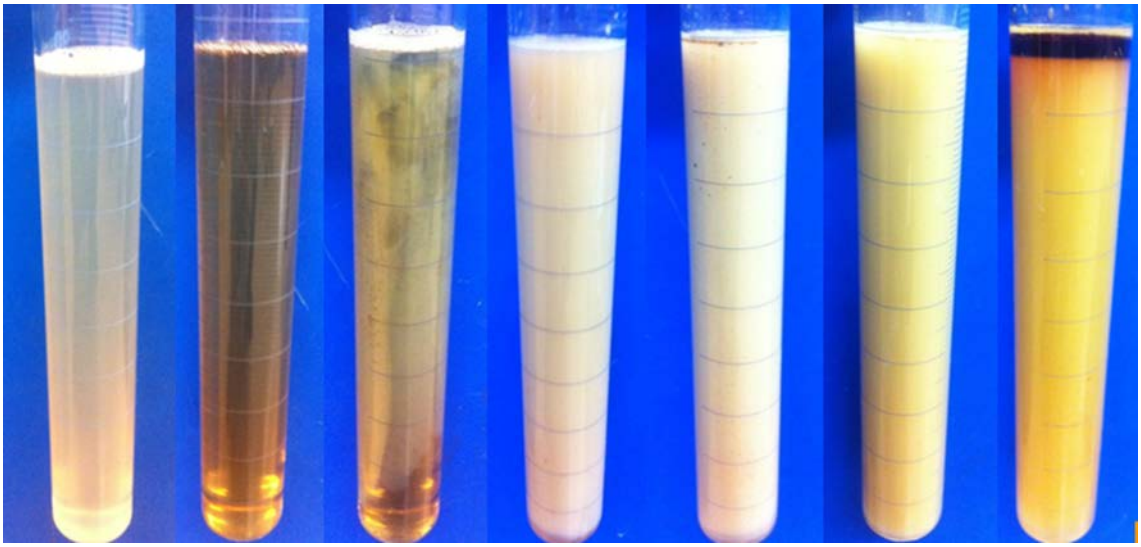

Fig. 24—4 wt% VES-based acid sample after hydrolysis of 0, 0.25, 0.5, 1, 2, 3, 6 hours separately at 250°F.

Photos of 4 wt% VES-based acid samples after hydrolysis of 0, 0.25, 0.5, 1, 2, 3, and 6 hours at 250°F are shown in **Fig. 24**. The fluid became progressively cloudy with an increase in hydrolysis time. Some samples had oil drops on the top, and the top oil layer became thicker. An apparent oil layer can be observed in the sample with 6-hour hydrolysis.

A drop of the substance from the top layer and the bottom layer were put into hexane and water separately. The top layer substance dissolved in hexane and the bottom layer substance dissolved in water. Therefore, the top layer substance is oil soluble, and the bottom layer substance is water soluble.

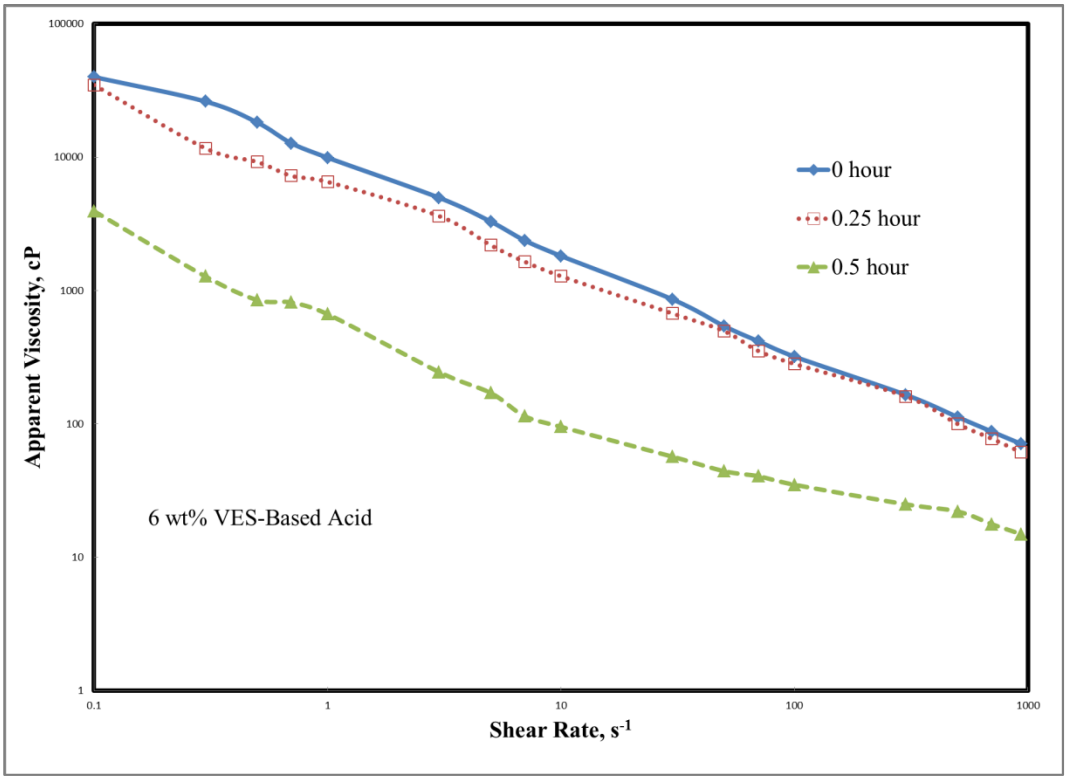

Fig. 25—Viscosity as a function of shear rates for 6 wt% VES-based acid (15 wt% HCl+ 1 vol% corrosion inhibitor) at 250°F, 300 psi.

Fig. 25 shows the trend of the 6 wt% VES-based acid viscosity change with shear rates under hydrolysis of 0, 0.25, and 0.5 hours at 250°F. (See more data for 4 wt% VES-based acid in **Table 9** in Appendix). In Fig. 25, 6 wt% VES acid systems, like the 4 wt% VES acid systems, had sample viscosities during the 0.25 hour hydrolysis that remained relatively high and constant at about 1500 cp, 520 cp, 300 cp and 160 cp at 10, 50, 100, 300 s^{-1}, respectively. After 0.25 hour, the viscosities greatly decreased, at 0.5 hour viscosities declined to around 30 cp, and at 1 hour, all of their viscosities were below 5 cp.

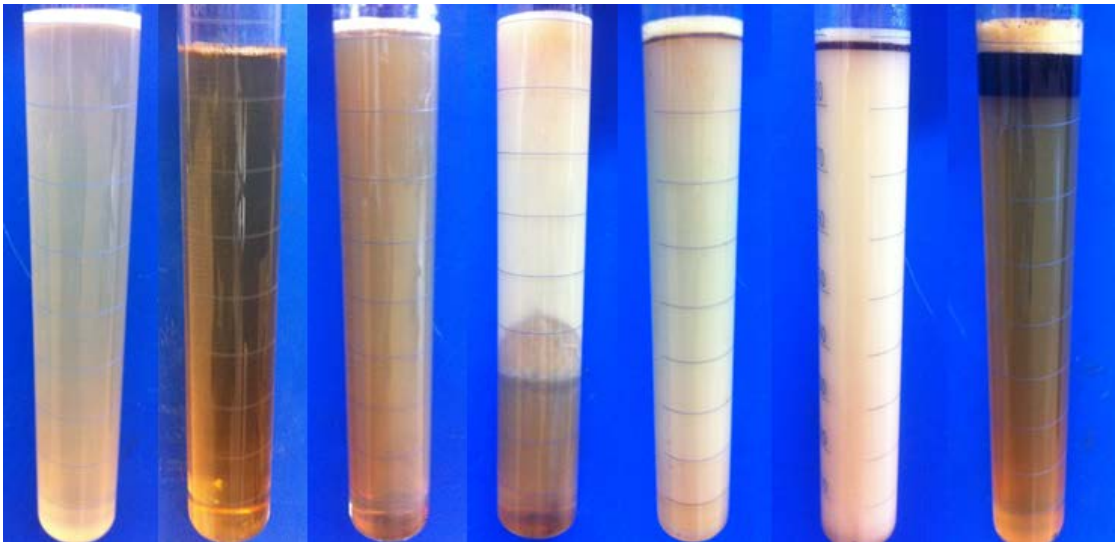

Fig. 26—6 wt% VES-based acid sample after hydrolysis of 0, 0.25, 0.5, 1, 2, 3, 6 hours separately at 250°F.

Fig. 26 shows the 6 wt% VES-based acid samples after the hydrolysis of 0, 0.25, 0.5, 1, 2, 3, and 6 hours at 250°F. From 0.5 hour to 3 hours, the samples become more and more opaque. And at 0.5 hour of hydrolysis, scattered oil drops start to appear. The top oil layers thickened with time. At 6 hours of hydrolysis, the top oil layer became very thick and the bottom layer became transparent.

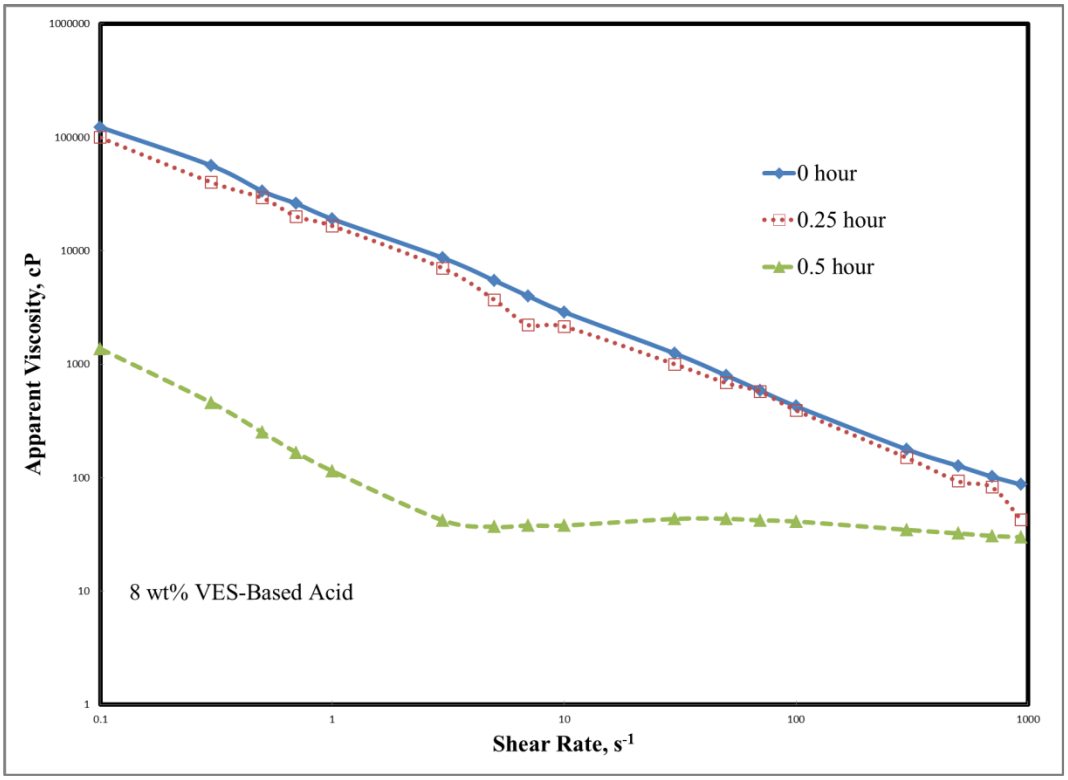

Fig. 27—Viscosity as a function of shear rates for 8 wt% VES-based acid (15 wt% HCl+ 1 vol% corrosion inhibitor) at 250°F, 300 psi.

Fig. 27 shows the trend of 8 wt% VES-based acid viscosity change with shear rates under hydrolysis of 0, 0.25, and 0.5 hour at 250°F. (See more data for 8 wt% VES-based acid in **Table 10** in the Appendix). As seen in Fig. 27, 8 wt% VES acid systems, similar to the 4 and 6 wt% VES acid systems, viscosities keep relatively high and stable at about 2500 cp, 750 cp, 420 cp, and 160 cp at 10, 50, 100, 300 s^{-1}, respectively for the first 0.25 hour hydrolysis and then decreased to around 30 cp at 0.5 hour. After 1 hour, the viscosities declined to below 5 cp.

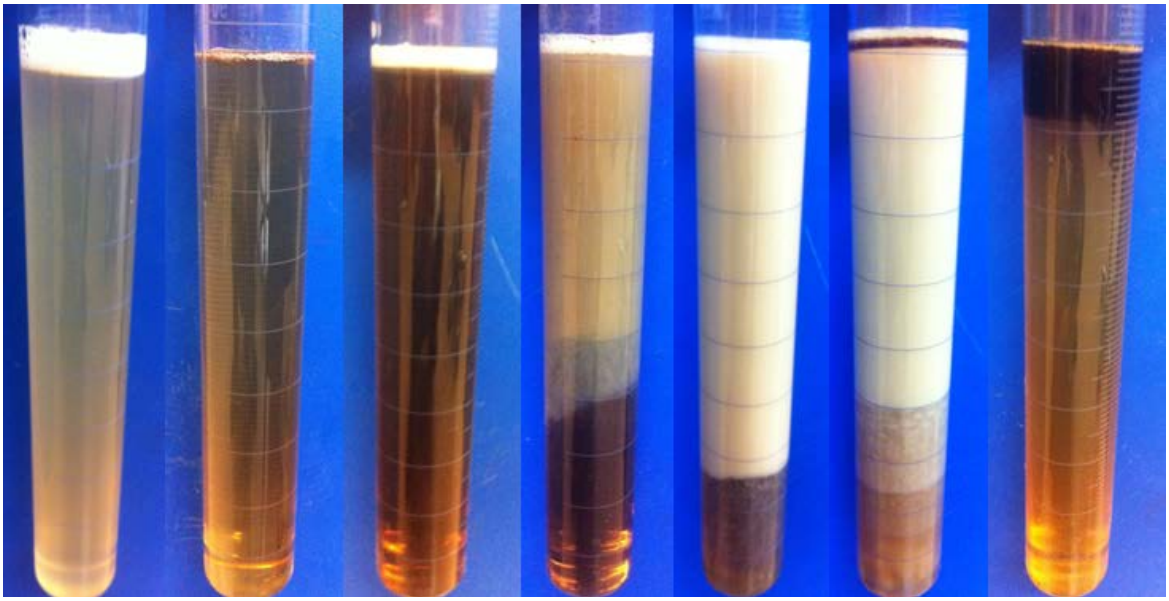

Fig. 28—8 wt% VES-based acid sample after hydrolysis of 0, 0.25, 0.5, 1, 2, 3, 6 hours separately at 250°F.

Fig. 28 shows 8 wt% VES sample after hydrolysis of 0, 0.25, 0.5, 1, 2, 3, and 6 hours separately at 250°F. The samples beome more and more cloudy with the increase of hydrolysis time. After 6 hours of hydrolysis, the oil layers become thicker and thicker with the increase in the concentration of the viscoelastic surfactant.

From Figs. 23, 25 and 27, we can conclude that for all samples with 15 wt% HCl, 1 vol% corrosion inhibitor and 4, 6, and 8 wt% viscoelastic surfactant hydrolyzed at 250°F and partially spent (pH 4.5) at 300 psia, the viscosity of the new VES-based acid remained high and stable during the first 15 minutes of hydrolysis, and relatively a big viscosity reduction occurred at 0.50 hour hydrolysis. When the see-through cell was first heated up to 200°F, and the samples were put into the cell under 300 psi, it took about 20 minutes for the temperature to rise from 200 to 250°F. When the hydrolysis experiment was over, it took about 10 minutes for the cell to cool down from 250 to

200°F. In order to accelerate the cooling, we used a wet, cold cloth to cool down the cell. The hydrolysis times were counted only when the temperature was at a stable 250°F.

As shown in **Figs. 29 and 30**, viscosity as a function of different hydrolysis times for different concentrations of VES-based acid at 100 s^{-1} and 300 s^{-1} is displayed. From these two figures, we can see much more clearly that the viscosity of the new VES-based acid remained fairly constant during the first 15 minutes of hydrolysis, and relatively a big viscosity reduction occurred at 0.50 hour hydrolysis. Viscosity decreased significantly after 1 hour of hydrolysis.

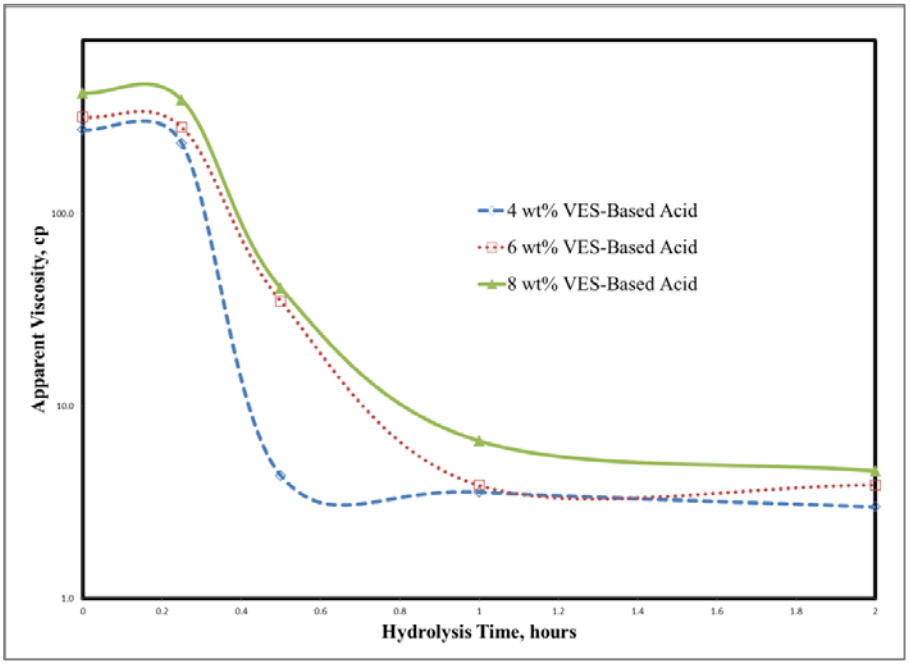

Fig. 29—Viscosity as a function of different hydrolysis time for different concentrations of VES-based acid (15 wt% HCl+ 1 vol% corrosion inhibitor) at 100 s^{-1} at 250°F, 300 psi.

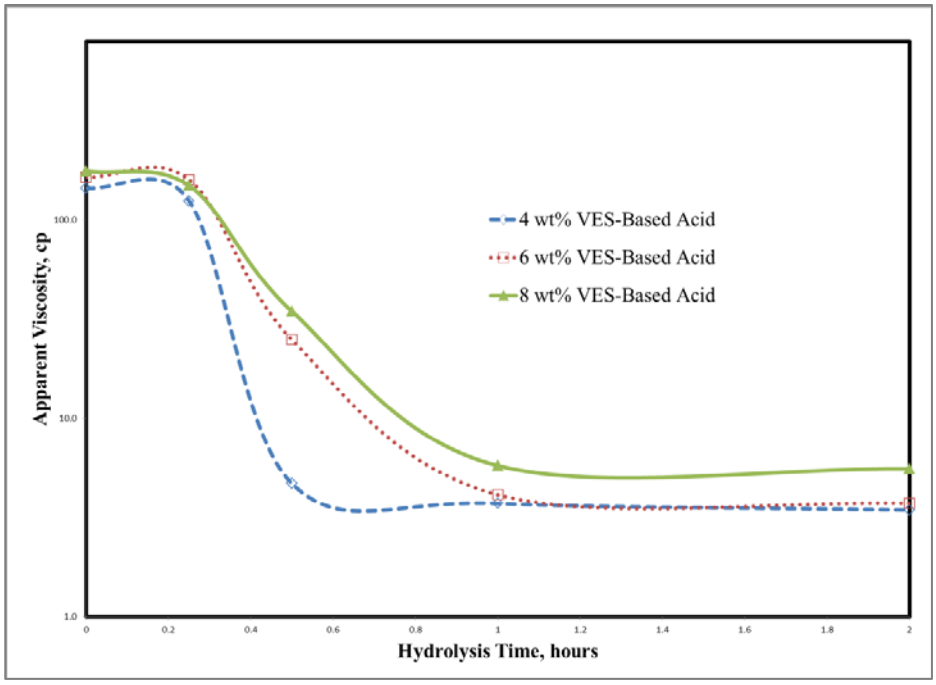

Fig. 30—Viscosity as a function of different hydrolysis time for different concentrations of VES-based acid (15 wt% HCl+ 1 vol% corrosion inhibitor) at 300 s^{-1} at 250°F, 300 psi.

The reaction products of the hydrolysis test at 250°F were qualitatively analyzed by mass spectrometry (MS). Electrospray ionization was performed using an Applied Biosystems QSTAR Pulsar (Concord, Canada). Solution was flowed at 7 ml/min through a 50-lm ID fused-silica capillary. Electrospray needle voltage was held at 4,500 V in positive mode and -4,500 V in negative mode. Nebulizer and curtain gas flow rates were held at 40 and 20 psi, respectively.

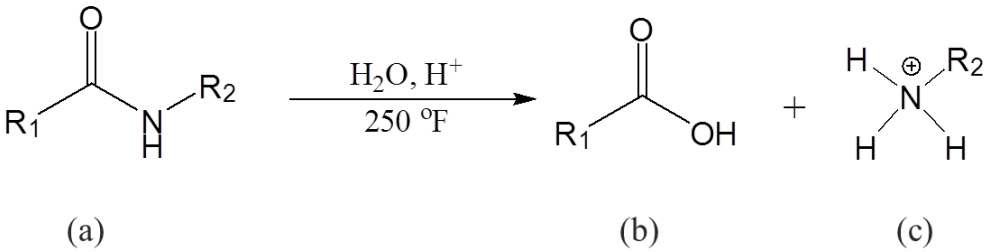

Fig. 31—Hydrolysis reaction of (a) the new VES into (b) fatty acid and (c) amine-based molecule.

In the samples hydrolyzed for 6 hours at 250°F, the upper layer of the sample was a viscous organic phase. The amount of the organic phase increased with the initial surfactant concentration. The lower layer was an aqueous phase. MS results showed that the organic phase consisted of the hydrophobic reaction product, a kind of fatty acid (**Fig. 31 (b)**). A peak in **Fig. 32** with high relative intensity was observed which corresponded well with its molecular weight. The hydrophilic reaction product in the aqueous phase had a peak (in **Fig. 33**) of MS relative intensity which was the molecular weight of amine-based molecule (**Fig. 31 (c)**).

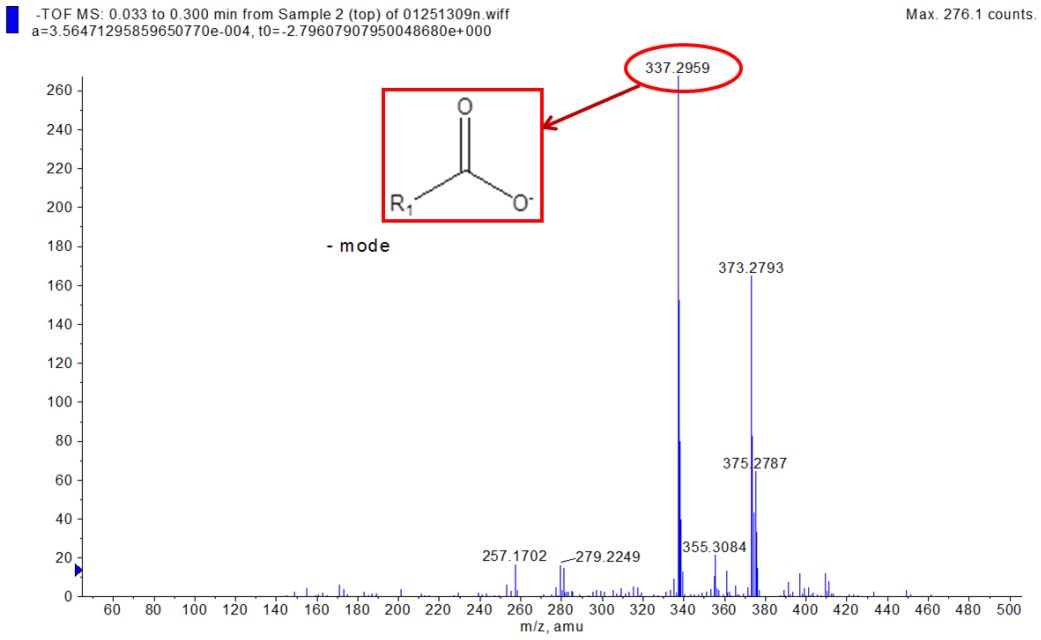

Fig. 32—Diagram of MS spectrum of top layer substances after 6 hours hydrolysis at 250°F with the range of 10 to 500 m/z.

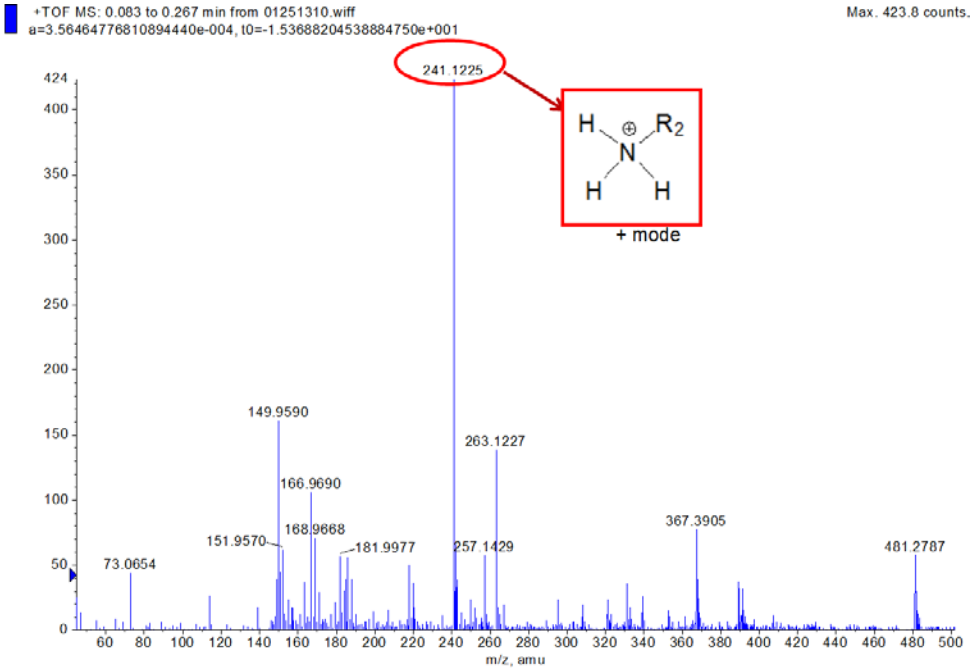

Fig. 33—Diagram of MS spectrum of bottom layer substances after 6 hours hydrolysis at 250°F with the range of 10 to 500 m/z.

From Figs. 24, 26, and 28, we can see that the samples became more and more cloudy, and finally apparent phase separation occurred. **Fig. 34** shows the lower cloudy part of the sample under the microscope. It is emulsion. A conductivity meter was used to measure the conductivity of the solution of the lower cloudy part. The results showed the sample was highly conductive. So, this is emulsion in which the continuous phase is water and the dispersed phase is fatty acid surrounded by the surfactants which can act as emulsifier. The samples in Figs. 24, 26, and 28 became more and more cloudy because more and more fatty acid was produced as hydrolysis went on; surfactants surrounded them to form emulsion and the concentration of the dispersed phase in the solution became progressively large. Hydrolysis continued, and fewer surfactants were left to work as emulsifiers. Finally, the emulsion broke down, and the fatty acid was released. It floated to the top of the solution forming the organic phase, and phase separation occurred.

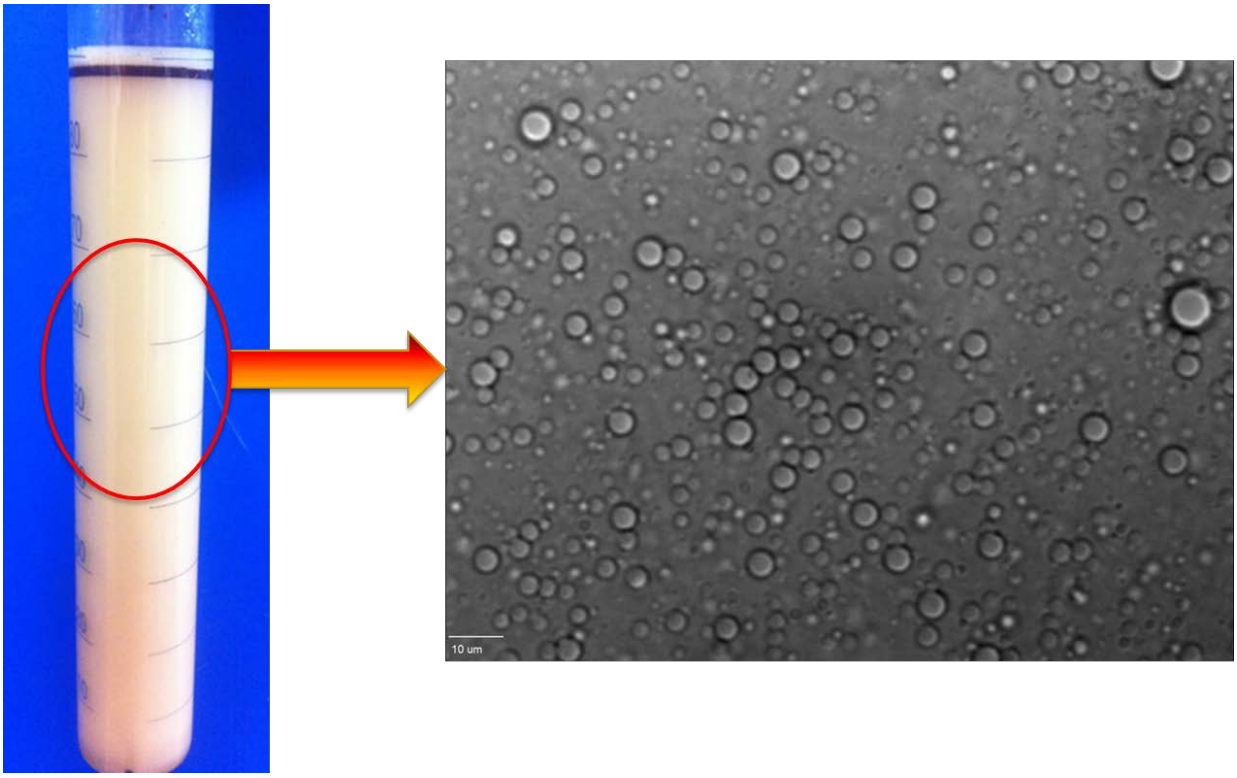

Fig. 34—The highly conductive, lower, cloudy part of the solution after 3 hours hydrolysis under the microscope.

CHAPTER III

COREFLOOD EXPERIMENT ON FORMATION DAMAGE CAUSED BY HYDROLYSIS PRODUCTS*

III.1 Materials

The materials used in this study are the VES sample (used as received), hydrochloric acid (ACS reagent grade, 36.7%), corrosion inhibitor, and Indiana limestone cores. Each sample was prepared with deionized water (resistivity = 18.2 MΩ·cm at 25°C).

III.2 Experiment Procedures

1. The Indiana limestone cores were cut into cylinders of 1.5 in. diameter and 6 in. length by using a drill press machine.
2. They were dried at 100°C for 3 hours and weighed to obtain their dry weights. Then they were saturated with DI water under vacumm for 4 hours to get their wet weights.
3. VES-based solutions were prepared such that HCl concentration was 15 wt%, corrosion inhibitor was 1 vol%, and the VES concentrations were 6 wt%.

---

* Parts of this chapter are reprinted with permission from "Hydrolysis Effect on the Properties of a New Class of Viscoelastic Surfactant-Based Acid and Damage Caused by the Hydrolysis Products" by Zhenhua He, Guanqun Wang, Hisham A. Nasr-El-Din, and Stuart Holt, 2013. Proceedings of SPE European Formation Damage Conference and Exhibition, Copyright [2013] by Society of Petroleum Engineers.

4. A core was placed inside the core holder (**Fig. 35**). Then the DI water was injected at different rates. According to the obtained pressure drops, the initial permeability of the core can be calculated.

5. When the temperature was stabilized at 250°F, the VES-based acid was injected into the core at 2.5 cm^3/min. After injecting 0.25 PV of the solution, it was kept inside core cylinder for 0 and 2 hours, respectively.

6. Backflow was applied with 10 vol% mutual solvent at the same rate until the pressure drop across the core was stable.

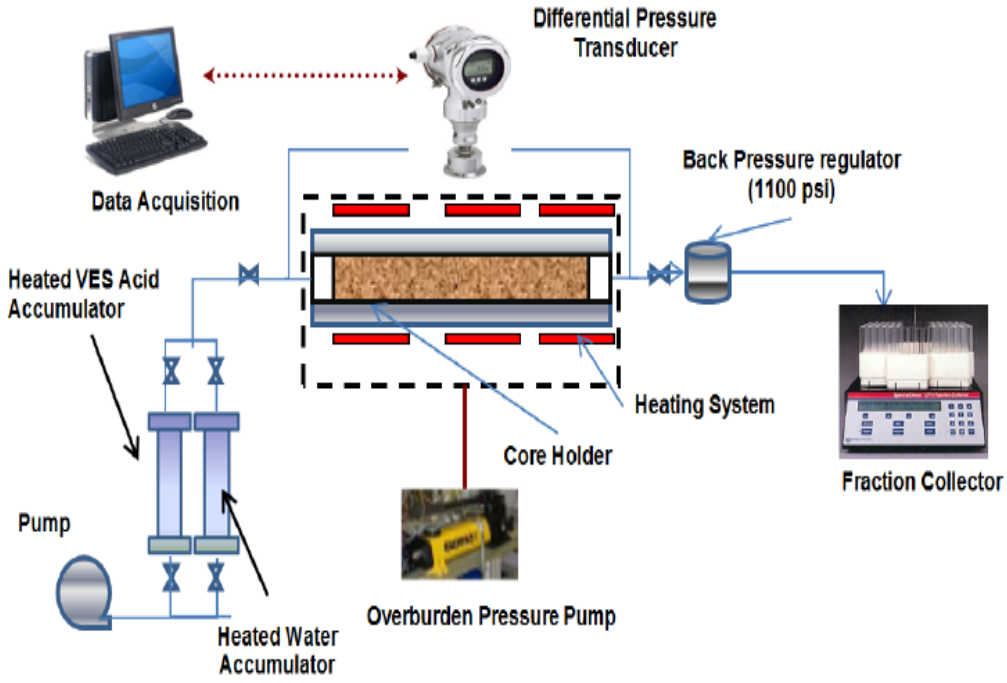

Fig. 35—Coreflood setup.

III.3 Results and Discussion

In the 0-hour hydrolysis coreflood experiment (the VES-based acid solution was not soaked inside the core), the initial permeability of the core used in this experiment was 177.0 md. After injecting 0.25 PV VES-based acids at 250°F, the VES-based acid was flushed back with 10 vol% mutual solvent. **Fig. 36** shows the inlet and outlet face of the 6-inch Indiana limestone core before and after the test with the VES-based acid solution (heated 0 hour at 250°F). **Fig. 37** shows the pressure drop across the core during the coreflood test.

Fig. 36—Inlet and outlet faces of the 6-inch Indiana limestone core before and after testing with the VES-based acid solution (heated 0 hour at 250°F).

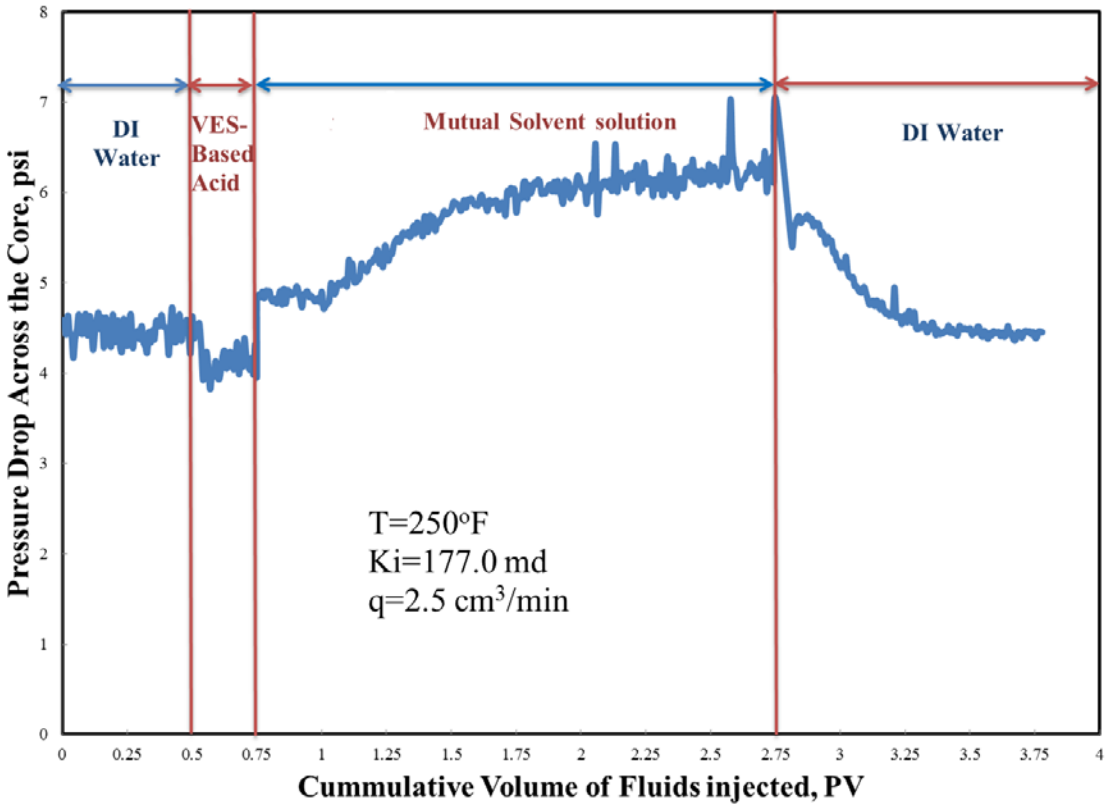

Fig. 37—Pressure drop across the core during the coreflood test.

When the VES-based acid was injected into the core, the VES-based acid was more viscous than the water. This would cause pressure buildup. However, the injection flow rate was 2.5 cm^3/min and only 0.25 PV fluid was injected, the injection time was so short that no significant gel was formed. On the other hand, the reaction between the Indiana limestone and the HCl at 250°F was fast enough to create many more spaces inside the core. Therefore, the pressure drop change should be influenced by these factors. Then the pressure started to build up because the 10 vol% mutual solvent was more visous. After this, the pressure drop decreased because the injection fluid was

switched to DI water. The final permeability of the core became 93.6 md (The results are shown in **Table 4**). The decreased permeability of the core sample indicated that some viscoelastic surfactant gel (see **Fig. 38**) stayed inside the core, blocked the pore throat and made the fluid flow harder. This caused formation damage with a 47.1% reduction in permeability.

Table 4—RESULTS OF THE COREFLOOD EXPERIMENTS

Core	k_i, md	PV, cm^3	T, °F	PV_{inj}, cm^3	t_{soak}, hrs	k_f, md	k_f/k_i
#1	177.0	26.64	250	6.66	0	93.6	0.529
#2	145.5	26.27	250	6.57	2	251.9	1.731

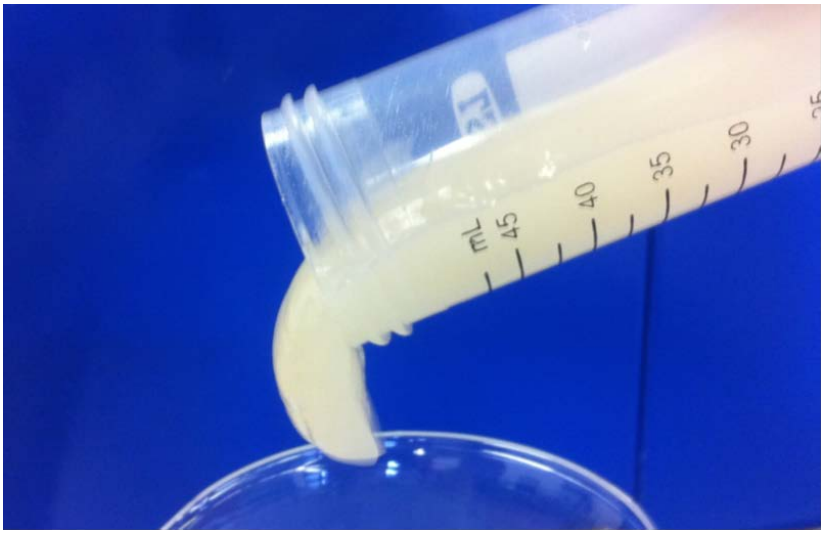

Fig. 38—Viscoelastic surfactant gel formed by 6 wt% VES-based acid after 0 hour of hydrolysis and neutralization with calcium carbonate powder.

In the 2-hour hydrolysis coreflood experiment, the VES-based acid solution was soaked inside the core for 2 hours. The initial permeability of the core was 145.5.0 md. After injecting 0.25 PV VES-based acid at 250°F, and soaking for 2 hours, the VES-based acid was flushed back with 10 vol% mutual solvent**. Fig. 39** shows the inlet and outlet face of the 6-inch Indiana limestone core before and after the test with the VES-based acid solution (heated 2 hours at 250°F). **Fig. 40** shows the pressure drop across the core during the coreflood test. The final permeability of the core became 251.9 md. The permeability was increased by 73.1%. After 2 hours of hydrolysis, most of the viscoelastic surfactants in the solution was hydrolyzed, and the fluid viscosity significantly decreased. It is much easier for the fluid to flow back rather than stay in the pores blocking the fluid flow.

When the acid reacts with the rock, it dissolves the rock and creates more pore space, and the permeability will be increased. In the beginning stages, viscoelastic surfactants in the acid fluid act as diverting agents when their viscosities are high. At this time, most of them work as viscous gel. If we had tried to flush them back at this time, a considerable amount of VES would have stayed inside the core and would have caused formation damage. However, if an appropriate time is selected to flow them back when most of them have hydrolyzed, the residual left in the reservoir will be much less, and the permeability will be increased.

Fig. 39—Inlet and outlet faces of the 6-inch Indiana limestone core before and after testing with VES-based acid solution (heated 2 hours at 250°F).

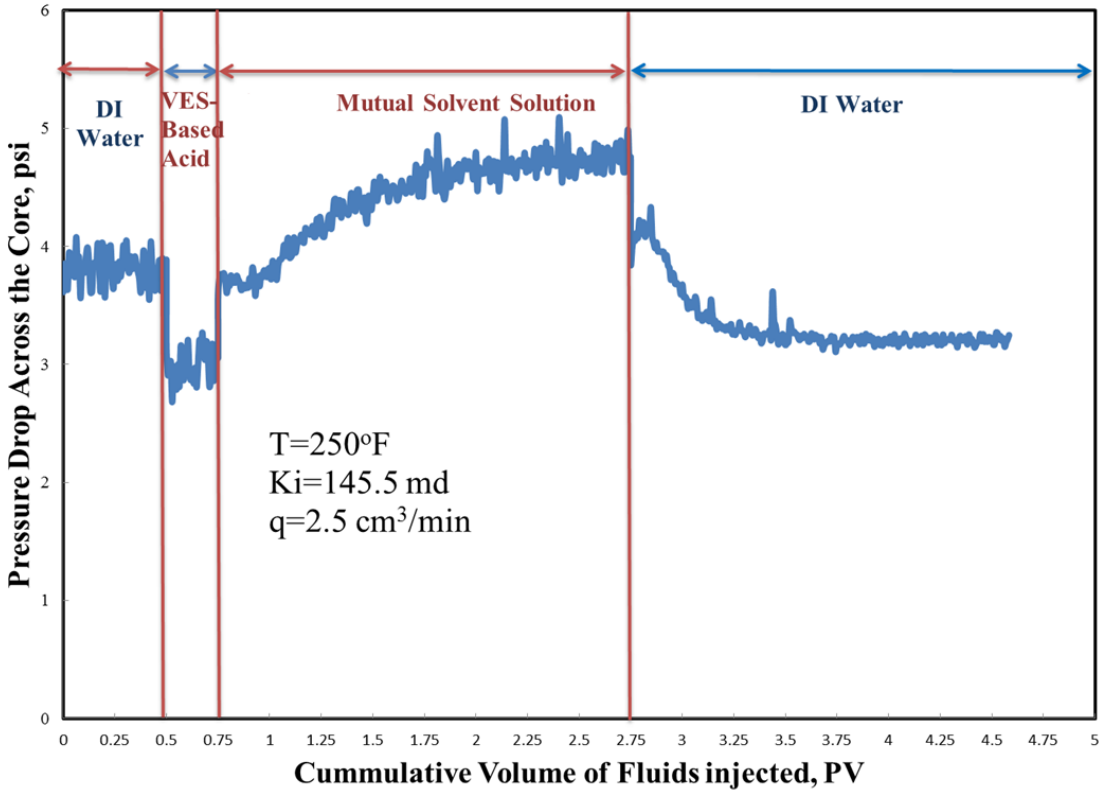

Fig. 40—Pressure drop across the core during the coreflood test.

CHAPTER IV

CONCLUSIONS*

In this study, the viscosity change of the VES-based acid was measured under different shear rates and at different hydrolysis times, mass spectrometry (MS) was used to analyze the hydrolysis products of the VES, and the potential formation damage caused by the hydrolysis products was evaluated by conducting coreflood experiments. The conclusions are as follows:

1. At the temperature of 190°F and without any corrosion inhibitor, the viscosity of this VES-based acid remained relatively high during the first hour of hydrolysis and experienced a significant decrease after 2-3 hours of hydrolysis.
2. At the temperature of 250°F and with corrosion inhibitor, the viscosity of this VES-based acid remained relatively high during the first 0.25 hour of hydrolysis and experienced a significant decrease after that.
3. MS results showed that the hydrolysis reaction occurred at the peptide bonds. Phase separation was observed. The upper phase was formed by fatty acids, and amine-based molecules existed in the lower aqueous phase.

---

* Parts of this chapter are reprinted with permission from "Hydrolysis Effect on the Properties of a New Class of Viscoelastic Surfactant-Based Acid and Damage Caused by the Hydrolysis Products" by Zhenhua He, Guanqun Wang, Hisham A. Nasr-El-Din, and Stuart Holt, 2013. Proceedings of SPE European Formation Damage Conference and Exhibition, Copyright [2013] by Society of Petroleum Engineers.

4. Coreflood tests showed that if flow back of the VES-based acid occurred at an appropriate time, the acidizing treatment would increase the reservoir permeability rather than cause formation damage.

REFERENCES

Al-Muhareb, M.A., Nasr-El-Din, H.A., Samuel, E., Marcinew, R.P., and Samuel, M. 2003. Acid Fracturing of Power Water Injectors: A new Field Application Using Polymer-Free Fluids. Paper SPE 82210 presented at the SPE European Formation Damage Conference, The Hague, Netherlands, 13-14 May.

Artola, P., Alvarado, O., Huidobro, E., and Salmoran, A. 2004. Nondamaging Viscoelastic Surfactant-Based Fluids Used for Acid Fracturing Treatments in Veracruz Basin, Mexico. Paper SPE 86489 presented at the SPE International Symposium and Exhibition on Formation Damage Control, Lafayette, Louisiana, 18-20 February.

Bulat, D., Chen, Y., Graham, M.K., Marcinew, R., Adeogun, G., Sheng, J., and Abad, C. 2008. A Faster Cleanup, Produced Water-Compatible Fracturing Fluid: Fluid Designs and Field Case Studies. Paper SPE 112435 presented at the SPE International Symposium and Exhibition on Formation Damage Control, Lafayette, Louisiana, USA, 13-15 February.

Bustos, O.A., Heiken, K.R., Stewart, M.E., Heiken, K., Bui, T., Mueller, P., and Lipinski, E. 2007. Case Study: Application of a Viscoelastic Surfactant-Based CO_2 Compatible Fracturing Fluid in the Frontier Formation, Big Horn Basin, Wyoming. Paper SPE 107966 presented at the Rocky Mountain Oil & Gas Technology Symposium, Denver, Colorado, U.S.A, 16-18 April.

Economides, M.J., Hill, A.D., and Ehlig-Economides, C. 1994. *Petroleum Production Systems*. Upper Saddle River, New Jersey: Prentice Hall, 392-403.

Economides, M.J., Nolte, K.G. 2000. *Reservoir Stimulation, 3rd Edition*. (hardbound)Wiley, NY and Chichester, England.

Fontana, C., Muruaga, E., Perez, D.R., Tecpetrol S.A., Cabazzoli, G., and Krenz, A. 2007. Successful Application of High-Temperature Viscoelastic Surfactant (VES) Fracturing Fluids under Extreme Conditions in Patagonian Wells, San Jorge Basin. Paper SPE 107277 presented at the EUROPEC/EAGE Conference and Exhibition, London, U.K, 11-14 June.

Fu, D. and Chang, F. 2005. Compositions and Methods for Treating a Subterranean Formation. US Patent No. 6,929,070.

Fu, D. and Chang, F. 2006. Compositions and Methods for Treating a Subterranean Formation. US Patent No. 7,028,775.

Jahnke, R.W. 1977. Thickened Aqueous Compositions for Well Treatment. US Patent No. 4,061,580.

Kefi, S., Lee, J., Eric, N., Hernandez, A.N. et al. 2005. Expanding Applications for Viscoelastic Surfactants.

Li, L., Nasr-El-Din, H.A., and Cawiezel, K.E. 2010. Rheological Properties of a New Class of Viscoelastic Surfactant. *SPE Production & Operations* **25**(3): 355-366.

Li, L., Nasr-El-Din, H.A., Crews, J.B., and Cawiezel, K.E.. 2011. Impact of Organic Acids/Chelating Agents on the Rheological Properties of an Amidoamine-Oxide Surfactant. *SPE Production & Operations* **26**(1): 30-40.

Long, D.A. and Truscott, T.G. 1968. Peptide Kinetics, Part 6. Acid-Catalyzed Hydrolysis of Tetraglycine. *Trans. Faraday Soc*., **64**: 1624-1628.

Lynn, J.D. and Nasr-El-Din, H.A. 2001. A Core-Based Comparison of the Reaction Characteristics of Emulsified and In-Situ Gelled Acids in Low Permeability, High Temperature, Gas Bearing Carbonates. Paper SPE 65386 presented at the SPE International Symposium on Oilfield Chemistry, Houston, Texas, 13-16 February.

Muskat, M. 1949. *Physical Principles of Oil Production*. New York City: McGraw-Hill Book Co., Inc., 242.

Nasr-El-Din, H.A. and Al-Humaidan, A.Y. 2001. Iron Sulfide Scale: Formation, Removal, and Mitigation. Paper SPE 68315 presented at the SPE International Symposium on Oilfield Scale, Aberdeen, 30-31 January

Nasr-El-Din, H.A., Samuel, E., and Samuel, M. 2003. Application of a New Class of Surfactants in Stimulation Treatments. Paper SPE 84898 presented at the SPE International Improved Oil Recovery Conference in Asia Pacific, Kuala Lumpur, Malaysia, 20-21 October.

Nasr-El-Din, H.A., Taylor, K.C., and Al-Hajji, H.H. 2002. Propagation of Cross-Linkers Used in In-Situ Gelled Acids in Carbonate Reservoirs. Paper SPE 75257 presented at the SPE/DOE Improved Oil Recovery Symposium, Tulsa, 13-17 April.

Qian, Y., Engel, M.H., Macko, S.A., Carpenter, S. and Deming J.W. 1993. Kinetics of Peptide Hydrolysis and Amino Acid Decomposition at High Temperature.

Geochimica et Cosmochrmm Ada, **57**: 3281-3293.

Samuel, M., Card, R.J., Nelson, E.B., Brown, J.E., Vinod, P.S., Temple, H.L. Qu, Q., and Fu, D.K.. 1997. Polymer-Free Fluid for Hydraulic Fracturing. Paper SPE 38622 presented at the SPE Annual Technical Conference and Exhibition, San Antonio, Texas, 5-8 October.

Samuel, M., Marci, R., Al-Harbi, M. Samuel, E., Xiao, Z., Ezzat, A.M., Jarrett, C., Ginest, N.H., Bartko, K., Hembling, D, and Nasr-El-Din, H.A. 2003. A New Solids-Free Non-Damaging High Temperature Lost-Circulation Pill: Development and First Field Applications. Paper SPE 81494 presented at the Middle East Oil Show, Bahrain, 9-12 June.

Syrinek, A.R., Buggs, R.N., and Gabel, R.K. 1991. Inorganic Acid solution viscosifier and corrosion inhibitor and method. US Patent No. 5,009,799.

Taylor, K.C. and Nasr-El-Din, H.A. 2002. Coreflood Evaluation of In-Situ Gelled Acids. Paper SPE 73707 presented at the SPE International Symposium and Exhibition on Formation Damage Control, Lafayette, Louisiana, 20-21 February.

Taylor, K.C. and Nasr-El-Din, H.A. 2003. Laboratory Evaluation of In-Situ Gelled Acids for Carbonate Reservoirs. *SPE J.* **8** (4): 426-434.

Wikipedia, Surfactant. 2013. http://en.wikipedia.org/wiki/Surfactant.

Yang, J. 2002. Viscoelastic Wormlike Micelles and Their Applications. *Curr. Opin. Colloid Interface Sci*. **7**(5–6): 276–281.

Yeager, V. and Shuchart, C. 1997. In Situ Gels Improve Formation Acidizing. *Oil &Gas J.* **95** (3): 70-72.

Yu, Meng (2011). Propagation and Retention of Viscoelastic Surfactants in Carbonate Cores. Doctoral dissertation, Texas A&M University. Available electronically from http://hdl.handle.net/1969.1/ETD-TAMU-2011-05-9544.

Yu, M., Mu, Y., Wang, G., and Nasr-El-Din, H.A. 2012. Impact of Hydrolysis at High Temperatures on the Apparent Viscosity of Carboxybetaine Viscoelastic Surfactant-Based Acid: Experimental and Molecular Dynamics Simulation Studies. *SPE Journal* **17** (4): 1119-1130.

Zeiler, C., Alleman, D., and Qu, Q. 2004. Use of Viscoelastic Surfactant-Based Diverting Agents for Acid Stimulation: Case Histories in Gom. Paper SPE 90062 presented at the SPE Annual Technical Conference and Exhibition, Houston, Texas, 26-29 September.

APPENDIX

Table 5—4 wt% VES-Based Acid Viscosity Changes with Different Hydrolysis Times at Different Shear Rates (190°F)

shear rate, s^{-1}	4 wt% VES-Based Acid Viscosities, cp							
	0 hour	0.25 hour	0.50 hour	0.75 hour	1 hour	2 hours	3 hours	6 hours
0.1	34424.5	36137.6	34322.3	30440.9	27780.2	2817.9	1122.6	1728.9
1.0	8488.8	8672.6	8634.3	8114.5	6490.7	714.9	154.2	224.5
10.0	1258.4	1267.0	1246.9	1152.0	1092.4	183.2	14.1	22.6
30.0	492.2	505.3	498.7	481.1	496.2	97.1	7.6	9.2
50.0	321.5	332.2	327.1	330.0	310.4	73.8	5.9	6.1
100.0	183.5	185.3	187.5	233.9	217.7	51.7	5.0	4.9
300.0	79.6	82.7	82.3	114.8	91.7	30.6	5.1	4.3
500.0	57.3	58.2	58.4	70.1	59.2	24.6	5.2	4.4
700.0	46.2	48.4	48.2	51.5	47.7	21.9	5.5	4.7
900.0	39.6	41.6	40.2	44.8	38.9	20.1	5.9	5.0

Table 6—6 wt% VES-Based Acid Viscosity Changes with Different Hydrolysis Times at Different Shear Rates (190°F)

shear rate, s^{-1}	6 wt% VES-Based Acid Viscosities, cp							
	0 hour	0.25 hour	0.50 hour	0.75 hour	1 hour	2 hours	3 hours	6 hours
0.1	104686.1	107867.6	60196.6	65363.4	31291.9	2179.6	2079.2	1160.7
1.0	21521.1	21872.7	14040.9	14955.3	9144.0	230.2	229.9	179.7
10.0	2659.7	2671.7	2096.0	2037.3	1717.1	29.2	24.5	17.5
30.0	965.6	963.3	795.8	793.9	764.1	12.9	10.3	7.7
50.0	597.8	601.2	507.9	509.1	539.1	9.8	7.1	6.2
100.0	320.5	322.7	280.5	286.3	326.7	7.8	5.6	4.6
300.0	122.6	122.2	112.1	125.9	159.3	7.1	5.1	7.0
500.0	81.8	82.8	78.4	86.3	104.0	7.1	5.1	7.8
700.0	66.2	66.9	63.7	69.0	77.9	7.4	5.4	8.3
900.0	57.4	57.6	53.7	60.5	62.1	7.7	5.8	9.0

Table 7—8 wt% VES-Based Acid Viscosity Changes with Different Hydrolysis Times at Different Shear Rates (190°F)

shear rate, s^{-1}	8 wt% VES-Based Acid Viscosities, cp							
	0 hour	0.25 hour	0.50 hour	0.75 hour	1 hour	2 hours	3 hours	6 hours
0.1	165275.1	229364.8	141590.7	163018.0	115242.5	1422.5	1655.0	2001.1
1.0	27666.2	35312.2	28158.3	31536.9	23917.0	160.6	193.7	198.8
10.0	3271.2	4215.6	3252.7	3689.2	3463.1	16.3	20.8	22.0
30.0	1179.7	1520.3	1106.3	1299.1	1260.7	8.3	10.4	9.9
50.0	752.5	943.2	680.0	790.5	804.8	7.2	8.1	7.5
100.0	437.7	479.0	361.4	411.5	438.1	6.0	6.5	6.0
300.0	175.5	188.3	143.9	155.3	175.9	6.2	6.4	5.7
500.0	122.7	123.1	98.2	106.1	124.3	6.4	6.5	6.0
700.0	102.2	98.5	79.1	83.9	94.1	6.8	6.6	6.3
900.0	89.1	83.7	65.7	71.4	79.9	7.3	7.1	6.8

Table 8—4 wt% VES-Based Acid Viscosity Changes with Different Hydrolysis Times at Different Shear Rates (250°F, with Corrosion Inhibitor)

shear rate, s^{-1}	4 wt% VES-Based Acid Viscosities, cp						
	0 hour	0.25 hour	0.50 hour	1 hour	2 hours	3 hours	6 hours
0.1	23384.2	25707.7	2272.1	1309.1	836.6	1105.7	1041.0
1.0	6123.7	5436.6	192.2	120.6	110.1	112.2	98.9
10.0	1108.2	1090.8	13.9	11.7	6.7	9.6	8.4
30.0	539.0	538.0	6.3	5.3	4.0	3.9	3.7
50.0	317.5	300.2	4.9	4.0	3.4	3.3	3.2
100.0	274.3	232.9	4.3	3.6	3.0	3.1	2.7
300.0	145.3	125.4	4.7	3.7	3.5	3.5	3.1
500.0	89.2	70.4	5.2	4.2	4.1	4.0	3.6
700.0	69.3	45.2	5.8	4.6	4.4	4.2	4.0
900.0	51.0	42.1	6.4	5.2	4.9	4.8	4.5

Table 9—6 wt% VES-Based Acid Viscosity Changes with Different Hydrolysis Times at Different Shear Rates (250°F, with Corrosion Inhibitor)

shear rate, s^{-1}	6 wt% VES-Based Acid Viscosities, cp						
	0 hour	0.25 hour	0.50 hour	1 hour	2 hours	3 hours	6 hours
0.1	39948.5	34760.2	3934.2	1117.7	1162.3	1389.8	1214.1
1.0	9918.7	6529.7	665.8	122.4	119.5	142.3	131.2
10.0	1817.6	1281.8	95.1	8.6	10.7	11.3	10.7
30.0	859.4	673.6	56.8	5.2	4.8	5.2	4.8
50.0	541.0	496.2	44.2	4.5	4.6	3.9	4.1
100.0	319.7	281.8	35.0	3.9	3.9	3.5	3.1
300.0	165.1	160.6	25.0	4.1	3.7	3.8	3.3
500.0	112.6	99.8	22.1	5.3	4.5	4.0	3.7
700.0	87.6	77.5	17.7	5.9	4.8	4.4	4.0
900.0	70.8	61.3	14.9	6.2	5.5	5.0	4.6

Table 10—8 wt% VES-Based Acid Viscosity Changes with Different Hydrolysis Times at Different Shear Rates (250°F, with Corrosion Inhibitor)

shear rate, s^{-1}	8 wt% VES-Based Acid Viscosities, cp						
	0 hour	0.25 hour	0.50 hour	1 hour	2 hours	3 hours	6 hours
0.1	122689.2	99315.6	1367.8	1467.5	884.2	1524.9	469.4
1.0	19039.3	16543.5	114.4	153.2	37.0	159.6	45.6
10.0	2882.4	2146.0	37.9	35.6	3.0	17.8	3.9
30.0	1242.8	999.5	43.3	14.4	3.5	9.2	6.4
50.0	795.0	682.5	43.4	10.2	4.0	7.6	4.6
100.0	425.9	392.2	41.1	6.6	4.6	6.5	4.6
300.0	177.6	149.8	34.7	5.8	5.6	5.2	4.6
500.0	127.1	93.0	32.3	7.5	5.6	5.5	4.5
700.0	102.0	82.1	30.7	7.1	5.9	5.6	4.6
900.0	86.9	42.4	29.9	7.7	6.6	6.2	5.4